UNIVERSITY
of ALASKA

Many Traditions One Alaska
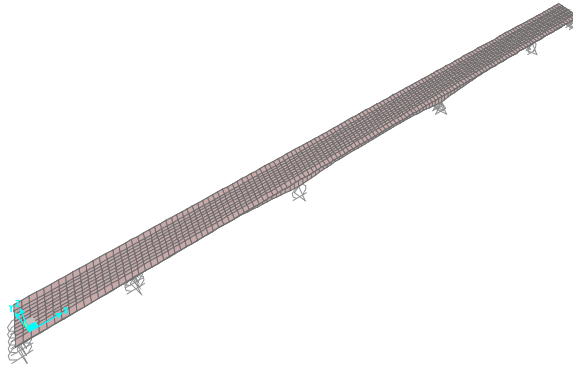
Phase II: Chulitna River Bridge Structurally Health Monitoring

Item Type	Technical Report
Authors	Hulsey, J. Leroy; Xiao, Feng; Dolan, J. Daniel
Download date	11/02/2021 19:17:07
Link to Item	http://hdl.handle.net/11122/10375

Phase II: Chulitna River Bridge Structurally Health Monitoring

Alaska Bridge 255 – Chulitna River Bridge

J. Leroy Hulsey, Ph.D., P.E., S.E.
Professor of Civil & Environmental Engineering
University of Alaska Fairbanks
Associate Director, Alaska University Transportation Center

Feng Xiao, Graduate Student
University of Alaska Fairbanks
Alaska University Transportation Center

J. Daniel Dolan, Ph.D., P.E.
Department of Civil & Environmental Engineering
Washington State University

January 2015

REPORT DOCUMENTATION PAGE

Form approved OMB No.

Public reporting for this collection of information is estimated to average 1 hour per response, including the time for reviewing instructions, searching existing data sources, gathering and maintaining the data needed, and completing and reviewing the collection of information. Send comments regarding this burden estimate or any other aspect of this collection of information, including suggestion for reducing this burden to Washington Headquarters Services, Directorate for Information Operations and Reports, 1215 Jefferson Davis Highway, Suite 1204, Arlington, VA 22202-4302, and to the Office of Management and Budget, Paperwork Reduction Project (0704-1833), Washington, DC 20503

1. AGENCY USE ONLY (LEAVE BLANK) 4000111b	2. REPORT DATE January 2015	3. REPORT TYPE AND DATES COVERED Final Report September 2012- December 2013

4. TITLE AND SUBTITLE	5. FUNDING NUMBERS
Phase II Chulitna River Bridge Structurally Health Monitoring	G8085 PACTRANS G8085 T2-11-08 4000111b

6. AUTHOR(S)
J. Leroy Hulsey, PhD., P.E., S.E. Feng Xiao, Graduate Student J. Daniel Dolan, PhD., P.E.

7. PERFORMING ORGANIZATION NAME(S) AND ADDRESS(ES)	8. PERFORMING ORGANIZATION REPORT NUMBER
Alaska University Transportation Center University of Alaska Fairbanks Duckering Building Room 245 P.O. Box 755900 Fairbanks, AK 99775-5900	INE/AUTC 14.04

9. SPONSORING/MONITORING AGENCY NAME(S) AND ADDRESS(ES)	10. SPONSORING/MONITORING AGENCY REPORT NUMBER
State of Alaska, Alaska Dept. of Transportation and Public Facilities Research and Technology Transfer 2301 Peger Rd Fairbanks, AK 99709-5399	T2-11-08 4000111b

11. SUPPLENMENTARY NOTES

12a. DISTRIBUTION / AVAILABILITY STATEMENT No restrictions	12b. DISTRIBUTION CODE

13. ABSTRACT (Maximum 200 words)

This study is phase 2 of a two phase research project. In Phase 1 a structural health monitoring system (SHMS) was installed on the Chulitna River Bridge. This bridge is 790 feet long, 42 foot 2 inches wide and has 5 spans. As part of that effort, three loaded dump trucks were used to conduct seventeen static and dynamic loadings on the structure. In addition to studying the bridge using SHMS, two ambient free vibration tests were conducted a year apart by.

In 1993, the deck on this 1970 five span bridge was widened from 34-feet to a 42 foot 2 inch concrete deck. Increased load was accounted for by strengthening two variable depth exterior girders and converting interior stringers to interior truss girders. Construction documents for the upgrade called for stage construction. At the time of this study, the bridge had five bearings that were not in contact with the superstructure.

Feasibility of using Structural Health Monitoring Systems (SHMS) for Alaska Highway Bridges was examined. Also, SHMS data for the load tests of Phase 1 were used to calibrate a three-dimensional model (FEM) to predict response and conduct a 2014 Operating Load Rating.

14- KEYWORDS : Instrumentation (Esxj), Sensors (Dmgu), Testing (G), Finite Element Method (Gej), Load factor, (Rkmyim), Structural health monitoring (Grs)	15. NUMBER OF PAGES 96
	16. PRICE CODE N/A

17. SECURITY CLASSIFICATION OF REPORT Unclassified	18. SECURITY CLASSIFICATION OF THIS PAGE Unclassified	19. SECURITY CLASSIFICATION OF ABSTRACT Unclassified	20. LIMITATION OF ABSTRACT N/A

NSN 7540-01-280-5500

STANDARD FORM 298 (Rev. 2-98)
Prescribed by ANSI Std. 239-18 298

SI* (MODERN METRIC) CONVERSION FACTORS

APPROXIMATE CONVERSIONS TO SI UNITS

Symbol	When You Know	Multiply By	To Find	Symbol
LENGTH				
in	inches	25.4	millimeters	mm
ft	feet	0.305	meters	m
yd	yards	0.914	meters	m
mi	miles	1.61	kilometers	km
AREA				
in^2	square inches	645.2	square millimeters	mm^2
ft^2	square feet	0.093	square meters	m^2
yd^2	square yard	0.836	square meters	m^2
ac	acres	0.405	hectares	ha
mi^2	square miles	2.59	square kilometers	km^2
VOLUME				
fl oz	fluid ounces	29.57	milliliters	mL
gal	gallons	3.785	liters	L
ft^3	cubic feet	0.028	cubic meters	m^3
yd^3	cubic yards	0.765	cubic meters	m^3
NOTE: volumes greater than 1000 L shall be shown in m^3				
MASS				
oz	ounces	28.35	grams	g
lb	pounds	0.454	kilograms	kg
T	short tons (2000 lb)	0.907	megagrams (or "metric ton")	Mg (or "t")
TEMPERATURE (exact degrees)				
^oF	Fahrenheit	5 (F-32)/9 or (F-32)/1.8	Celsius	^oC
ILLUMINATION				
fc	foot-candles	10.76	lux	lx
fl	foot-Lamberts	3.426	candela/m^2	cd/m^2
FORCE and PRESSURE or STRESS				
lbf	poundforce	4.45	newtons	N
lbf/in^2	poundforce per square inch	6.89	kilopascals	kPa

APPROXIMATE CONVERSIONS FROM SI UNITS

Symbol	When You Know	Multiply By	To Find	Symbol
LENGTH				
mm	millimeters	0.039	inches	in
m	meters	3.28	feet	ft
m	meters	1.09	yards	yd
km	kilometers	0.621	miles	mi
AREA				
mm^2	square millimeters	0.0016	square inches	in^2
m^2	square meters	10.764	square feet	ft^2
m^2	square meters	1.195	square yards	yd^2
ha	hectares	2.47	acres	ac
km^2	square kilometers	0.386	square miles	mi^2
VOLUME				
mL	milliliters	0.034	fluid ounces	fl oz
L	liters	0.264	gallons	gal
m^3	cubic meters	35.314	cubic feet	ft^3
m^3	cubic meters	1.307	cubic yards	yd^3
MASS				
g	grams	0.035	ounces	oz
kg	kilograms	2.202	pounds	lb
Mg (or "t")	megagrams (or "metric ton")	1.103	short tons (2000 lb)	T
TEMPERATURE (exact degrees)				
^oC	Celsius	1.8C+32	Fahrenheit	^oF
ILLUMINATION				
lx	lux	0.0929	foot-candles	fc
cd/m^2	candela/m^2	0.2919	foot-Lamberts	fl
FORCE and PRESSURE or STRESS				
N	newtons	0.225	poundforce	lbf
kPa	kilopascals	0.145	poundforce per square inch	lbf/in^2

*SI is the symbol for the International System of Units. Appropriate rounding should be made to comply with Section 4 of ASTM E380.
(Revised March 2003)

TABLE OF CONTENTS

LIST OF FIGURES

LIST OF TABLES

DISCLAIMER

The contents of this report reflect the views of the authors, who are responsible for the facts and the accuracy of the information presented herein. This document is disseminated under the sponsorship of the U.S. Department of Transportation's University Transportation Centers Program, in the interest of information exchange. The Pacific Northwest Transportation Consortium and the U.S. Government assume no liability for the contents or use thereof.

EXECUTIVE SUMMARY

This report presents the feasibility of using Structural Health Monitoring for Alaska and provides the 2014 Operating Load Rating for the Chulitna River Bridge. Also, this report presents the bridge response using a structural health monitoring system (SHMS) and the predicted response using a calibrated finite element model of the bridge. The Chulitna River Bridge is on the Parks Highway. This bridge is 790 feet long, 42 foot 2 inches wide and has 5 spans.

Phase 1 (SHMS)

In Phase 1, the AUTC research team installed a SHMS on the Chulitna River Bridge (Hulsey, J.L., P. Brandon, and F. Xiao; 2012a). As part of the effort, the research team tested the bridge with dump trucks (2 bellies and 1 side dump) loaded with sand for17 different static and dynamic load combinations. Load tests were conducted to evaluate the structural performance against known measured values (Hulsey, J.L., P. Brandon, and F. Xiao., 2012d).   During installation of the SHMS, the AUTC team also installed 15 temporary accelerometers and monitored the ambient frequency response.

Phase 2 (Bridge Evaluation)

In 1993, the deck on this 1970 five-span bridge was widened from a 34-foot cast-in-place concrete deck to a 42-foot 2-inch concrete deck made of precast concrete deck panels. At the time, increased load was accounted for by strengthening two variable depth exterior girders and converting W21x44 interior stringers to an interior truss girder; the W21x44 became the upper chord of the truss. Construction documents for this upgrade called for stage construction. What is not known is how the support structure was assembled and if stresses were induced by traffic. Project engineer records for the 1993 widening were requested from the ADOT&PF archives but none were found. Thus, for the purpose of this study, structural dead load was assumed to be the as-built member weights.

Phase 2 findings:

(a) Structural Health Monitoring is a feasible method for monitoring long-term structural response. This recommendation is based on the idea that only the minimum number of stable long-term monitoring sensors should be used to address the purpose. Also, in Alaska (because of weather and remoteness) it is important that the monitoring system be

located off of the bridge at a centralized site such as the Bridge Design Office;

(b) A load rating for the Chulitna River Bridge was performed in accordance with LRFR AASHTO guidelines. The bridge passed the required Operating Load Rating (RF>1), and thereby posting will not be required. Although five support bearings at the piers are not in contact with the pier cap, experimental findings from static and dynamic load tests of Phase 1 showed that the bridge is performing satisfactorily. The following table illustrates the findings of the various Operating Load Rating options:

Summary of Load Ratings for Bridge Conditions

Load Type	Traffic Lanes	Analysis Conditions	Operating Load Rating		No. of Members with RF<1
			Member	RF	
HS20-44	3	Model 3 (6 members removed)	---	Passed	none
HL-93	3	Model 3 (6 members removed)	---	Passed	none
Permit	1	Model 3 (6 members removed)	'---	Passed	none

(c) Bridge response due to ambient frequency testing illustrated that no major changes occurred for the observational period; and

(d) Observational sensor response resulting from the SHMS monitoring of some permit loads indicated that the structure is responding satisfactorily.

CHAPTER 1.0 INTRODUCTION

1.1 History

Bridges in Alaska can be exposed to extremely cold temperatures and, depending on location, can be subjected to excessively deep snow, strong winds, and significant earthquake activity. Moreover, bridges in Alaska are often located in remote areas, and because of the harsh environment, maintenance and rehabilitation can be very expensive.

Asset management costs for maintenance, rehabilitation, and replacement depend on reliable inspection and condition assessment. Compared with other states, bridge monitoring in Alaska can provide cost savings and can be a valuable tool in evaluating structural condition. However, power and or phone service is not always available at a remote site, and this may be a challenge for real-time data retrieval.

In spring 2012, ADOT&PF selected the Chulitna River Bridge for study. One of the purposes for the study was to determine if a structural health monitoring system (SHMS) was appropriate for evaluating the state's bridges and if SHMS data would be reliable and of value to the department. Another purpose was to utilize what was learned through testing and monitoring and load rate the bridge. The bridge is located at Milepost 132.7 on the Parks Highway between Fairbanks and Anchorage, Alaska. This highway is the most direct route connecting Anchorage to Fairbanks and the oil fields in Prudhoe Bay. Because of oil field operational demands, overload vehicles up to 410,000 pounds travel over this bridge regularly. In 2004, ADOT&PF discovered five locations where the bridge superstructure did not sit on its support bearings. Some unusual features of this bridge and the fact that it is not supported as designed made it a likely candidate for evaluation.

1.2 Bridge Details

The Chulitna River Bridge was built in 1970 on a 22-degree skew. It is 790-feet long with five spans of 100, 185, 220, 185, and 100 feet. The superstructure was a 34-foot-wide by 6¾-inch-thick cast-in-place concrete deck supported by two exterior continuous longitudinal variable depth girders and three interior stringers. The girder stringers are spaced at 7 feet on center. The interior stringers are supported by a cross frame that is carried by the exterior girders. The cross frame was detailed to transfer dead loads and traffic loads to the exterior girders.

Interior stringers were W21x44, and the exterior girders had a variable depth web that varied from 84 inches deep in the first and fifth spans to 108 inches deep in the middle spans. At Piers 2 and 4, the exterior girder web has a haunch depth of 148 inches. At Pier 3, the exterior girder web has a haunch depth of 168 inches.

In 1993, the bridge deck was widened from a 34-foot cast-in-place concrete deck to a 42-foot 2-inch concrete deck made of precast concrete deck panels. The minimum thickness of these concrete deck panels was 7½ inches; the maximum thickness was $8^{11}/_{16}$ inches. Increased future loads were accounted for by strengthening the variable depth exterior girders and converting the W21x44 interior stringers to interior truss girders; the W21x44 became the upper chord of the truss (see Figure 1.1).

Figure 1.1 Chulitna River Bridge, after 1993 upgrades

In September 2010, Bridge Diagnostics, Inc. (BDI) load tested the bridge. The primary goal of that test was to evaluate how the load is distributed from the driving surface into the support girders and cross frames. Test results were compared by HDR (consultants) with a finite element model. Some of the unique features of this bridge are that (a) the interior girders are substantially different from the exterior girders, and (b) that five rocker bearings are either not in contact or partially in contact with the masonry plates. Bearings not in contact with the bridge include three truss bearings at Pier 3 and two bearings at Pier 5 (see Figure 1.2.). Findings (by others) following that study led to a recommendation that the bridge should be posted.

Therefore, an additional study was introduced—a two-phase study; this report is Phase 2 of that study.
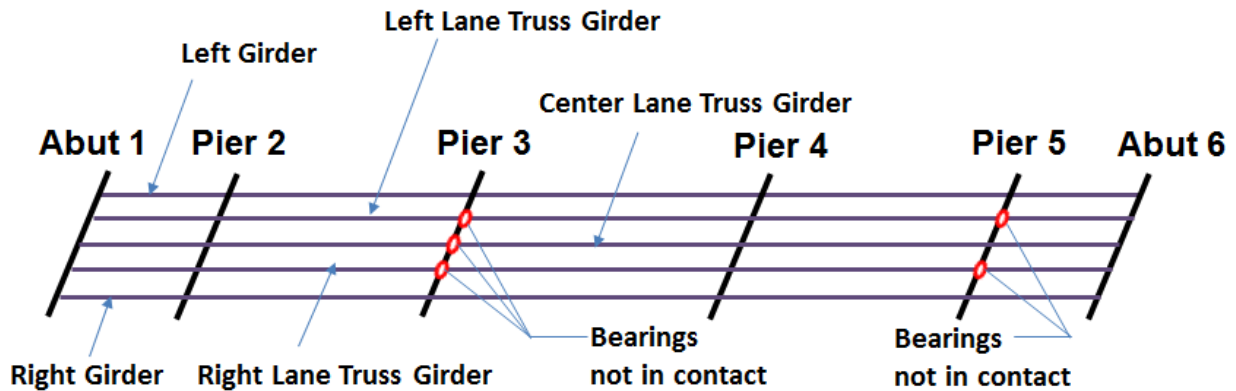
Figure 1.2 Plan view: Bearings that are not in contact with masonry plates

1.3 Phase 1 Research Study

In spring 2012, a research grant to UAF was jointly funded by ADOT&PF and AUTC to develop a SHMS that could be used to monitor Alaska bridges, instrument the bridge, calibrate the system, and load test the structure. Phase 1 was to be completed at or around the end of September 2012. Phase 1 involved selecting and installing a SHMS at the Chulitna River Bridge to monitor the bridge response to known truck loads crossing the structure. Phase 1 was completed in September 2012, and the reports on that phase are presented elsewhere.

1.4 Phase 2 Research Study

The ADOT&PF, AUTC, and PacTrans funded UAF and Washington State University (WSU) to monitor the bridge through December 31, 2013. In addition to monitoring bridge response to traffic, the research team was to develop and calibrate a finite element model that would provide a reliable bridge behavioral response to traffic, AASHTO loading, and special permitted vehicles. Part of the scope of the study was to load rate the bridge.

Experimental response data were obtained from two sources: the SHMS and a portable monitoring system in which 15 portable accelerometers were placed across the driving surface to monitor ambient accelerations.

Structural health monitoring can be used to provide early warnings about bridge safety and to monitor structural condition and changes in condition in real time, typically by monitoring

strain, acceleration, displacement, temperature, etc. Other uses include providing valuable data for engineers who are preparing asset management plans.

A three-dimensional finite element model (FEM) was calibrated to the load tests of Phase 1. Test results for the load tests of Phase 1 were compared and are presented in the Appendices of this report. Comparative results between FEM and experimental load test data were satisfactory and suggest (for the bridge's existing condition) that the finite model may be used to evaluate the Chulitna River Bridge behavior for a given set of traffic conditions.

CHAPTER 2.0 LOAD RATING

2.1   General

An operating load rating for the Chulitna River Bridge was performed in spring 2014. The rating was based on the LRFR method according to the AASHTO *Manual for Bridge Evaluation* (AASHTO, 2011) and design was checked in accordance with the LRFD Bridge Design Specifications (AASHTO 2012). Girders, composite trusses, and cross frames were rated.

The load rating in this report is for a bridge that was constructed in 1970 and upgraded in 1993. The bridge rating was performed using CSiBridge (2014) in collaboration with a calibrated SAP2000 (version 14, 2014) finite element model (FEM) studied in Phases 1 and 2. The FEM was calibrated against two different experimental data sets in conjunction with the as-built construction drawings (see Chapter 3 and Appendices A–E). Project engineer field notes for the 1993 construction upgrade work were requested from ADOT&PF archives; however, no records were found. So, <u>what is not known are the built-in dead load stresses resulting from the bridge widening and strengthening activities that occurred in 1993.</u>

For a detailed description of the Chulitna River Bridge, see Section 1.2, Bridge Details. Bridge construction details are illustrated in Figures 2.1 through 2.7.
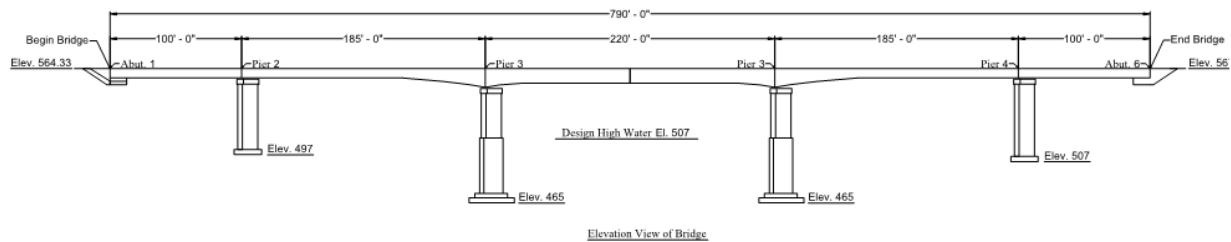
Figure 2.1 Elevation: Chulitna River Bridge
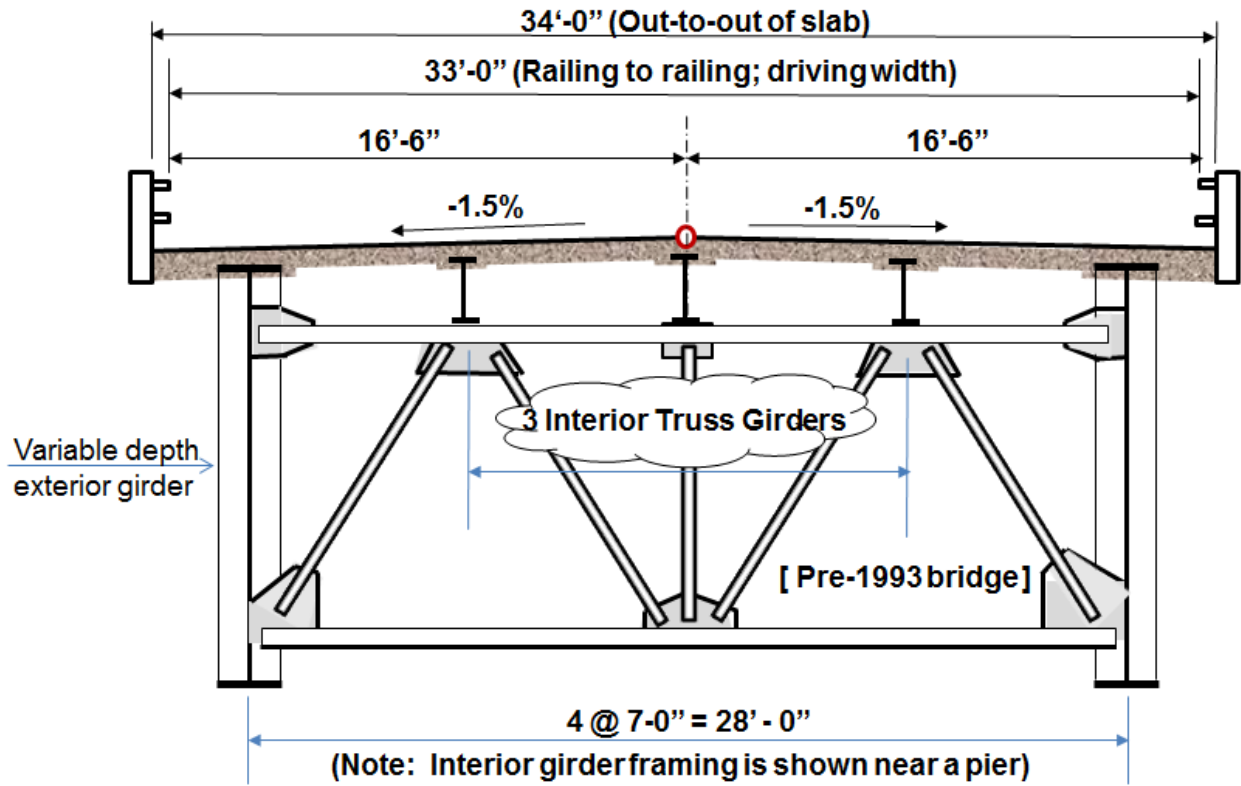
Figure 2.2 Bridge cross section (as-built in 1970)
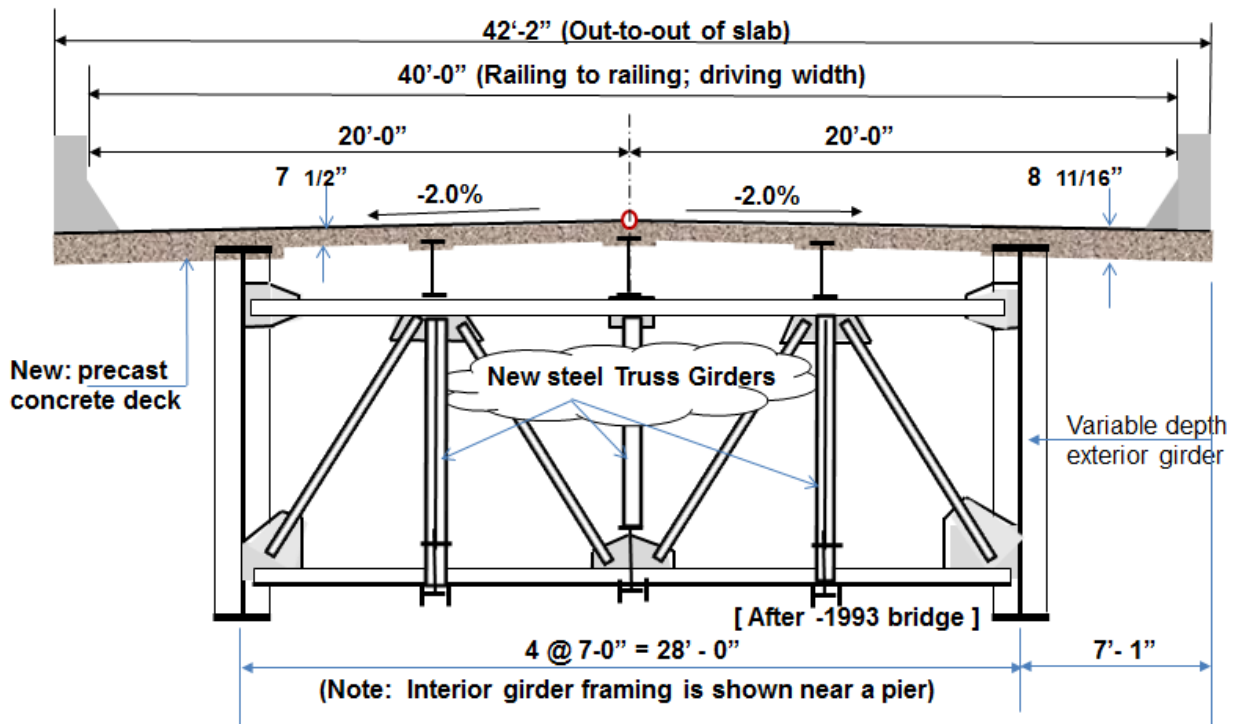
Figure 2.3 Bridge cross section (as-built in 1993)
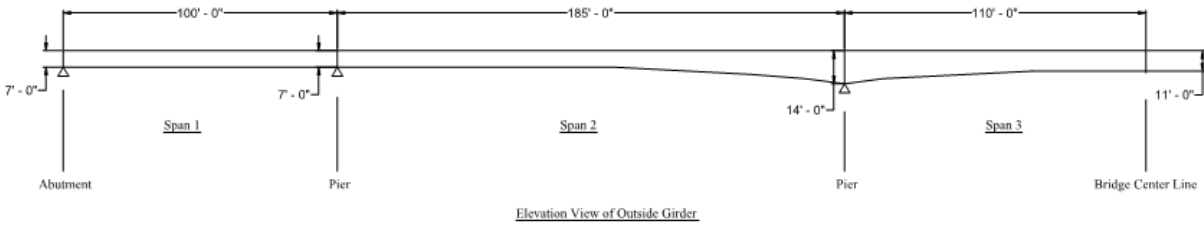
Figure 2.4 Elevation: Exterior variable depth girder
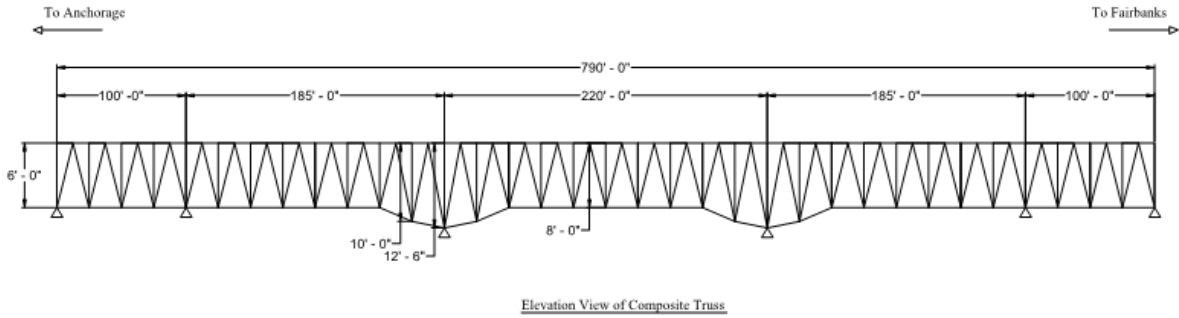
Figure 2.5 Elevation: Interior truss girder
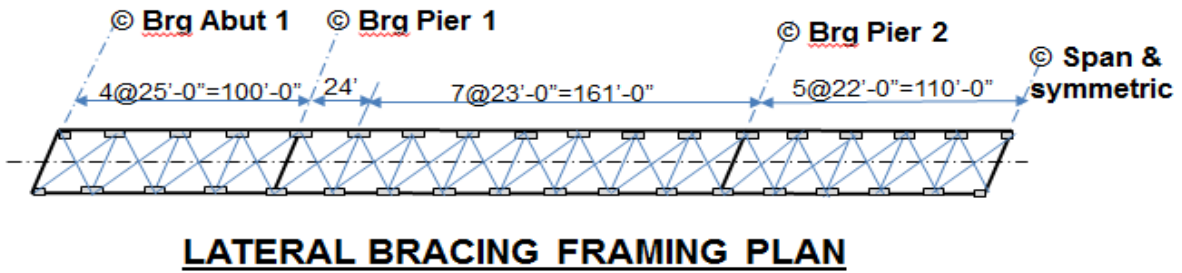
Figure 2.6 Plan: Lateral bracing for the superstructure
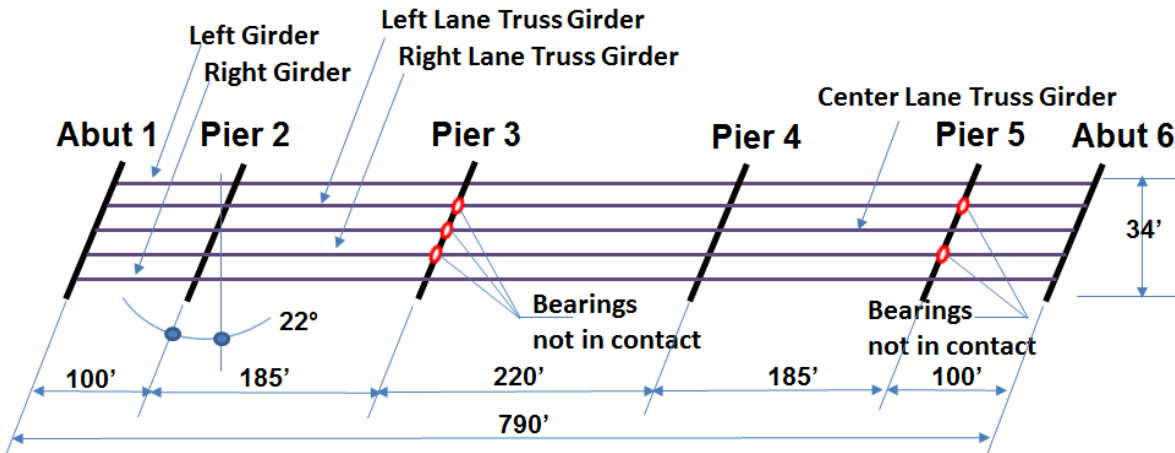
Figure 2.7 Plan: Bearing issue locations

2.2 Operating Load Rating

Member dead load stresses were based on the assumption that the structural framing was in place before the new deck and railings were installed; induced stresses caused by traffic may have occurred through stage loading was not accounted for. Operating load ratings were calculated in accordance with AASHTO (Steel Bridge Design Handbook, 2012) by using CSiBridge (2014) to meet the strength limit state (LRFR). Load ratings are provided for HL-93, HS20-44, and permit loads.

In accordance with AASHTO, the operating load rating for the "as-is" structure was evaluated for HL-93 loading on three (3) traffic lanes. Results showed four (4) members had an operating load rating less than 1; therefore, without strengthening or other alternatives the as-is bridge did not pass. Evaluation of the cause of the unsatisfactory load rating showed that members with less than satisfactory performance were secondary type members.

Subsequently, operating load ratings were calculated for (a) the bridge with all bearings supports in contact, and (b) secondary members removed from the structural analysis. The bridge operating load rating was evaluated for the following conditions, see Table 2.5:

1. HL-93 loading on three lanes (as-is condition);
2. HL-93 loading on two lanes (as-is condition);
3. HL-93 loading on two lanes (all bearing supports are in contact);
4. Permit truck on one lane (as-is condition);
5. HL-93 loading on three lanes (4, 5 and 6 secondary members removed);

6. HS20-44 loading on three lanes (4 and 5 secondary members removed);

7. HS20-44 loading on two lanes (4 and 5 secondary members removed); and

8. Permit trucks (as-is condition and 5 secondary members removed).

Detailed findings are presented in the following sections.

2.2.1 Investigation with updated calibrated finite element model (as-is condition)

The as-is 1993 bridge (condition simulated five bearing supports not in contact with pier cap supports). The structure was analyzed with an updated calibrated finite element model (FEM). This model was calibrated to the experimental data of Phase 1.

Three Traffic Lanes

- HL-93 loading on three traffic lanes had four members with an operating load rating below 1 ($LR < 1$). Four secondary members A, B, C, and D had load ratings below 1. These secondary members are not crucial to bridge safety (see Figure 2.8, Figures 2.23–2.24, and Table 2.1).

Two Traffic Lanes

- HL-93 loading on two traffic lanes had four members with an operating load rating below 1. Members with load ratings below 1 are A, B, C, and D and are secondary and not crucial to bridge safety (see Figure 2.9, Figures 2.23–2.24, and Table 2.1).

- HL-93 loading on two traffic lanes with all bearings in contact. One member, D, had an operating load rating below 1 (see Figure 2.10, Figure 2.24, and Table 2.1).

One Traffic Lane

- Permit loading on one traffic lane (truck is on the bridge centerline) produced an operating load rating below 1 ($RF < 1$) (see Figure 2.11, Figures 2.23, and Tables 2.1 and 2.2).

2.2.2 Model 1 – Four members (A, B, C, and D) removed

Four members—A, B, C, and D—were removed from the 1993 updated calibrated bridge model, and the structure was analyzed for the following conditions:

- HL-93 loading on three traffic lanes: Results showed an additional member (E) had a load rating below 1 (see Figure 2.12, Figures 2.23–2.24, and Table 2.3).

2.2.3 Model 2 – Five members (A, B, C, D, and E) removed

The bridge structure was analyzed to determine those members with load ratings of less than 1 ($RF < 1$). The following conditions were examined:

Three Traffic Lanes

- HL-93 on three traffic lanes: The operating load rating passed (see Figure 2.13, Figures 2.23–2.24, and Table 2.3).

- HS20-44 loads on three traffic lanes: The operating rating passed (see Figure 2.14, Figures 2.23–2.24, and Table 2.3).

Two Traffic Lanes

- HL-93 on two traffic lanes: Secondary member (F) had a rating of less than 1 (see Figure 2.15, Figures 2.22–2.24, and Table 2.3).

One Traffic Lane

- Permit loading on one traffic lane (truck is on the bridge centerline) passed the load rating test (see Figure 2.16, Figures 2.23–2.24, Tables 2.2 and 2.3).

2.2.4 Other alternative operating load ratings

- The bridge was analyzed using Model 2 (five removed members, A–E) for HL-93 loading on three traffic lanes. Sensitivity of the structure was examined; that is, $1 \leq RF < 1.25$ was used to evaluate truss member sensitivity for this structure. Four members (F–I) were found to meet this criteria. Member F had a load rating slightly larger than 1 ($RF = 1.01$) (see Figure 2.17, Figures 2.22–2.24, and Table 2.4).

- The bridge was analyzed using Model 2 (five removed members, A–E) for permit loading on one lane (truck on the centerline of the bridge) (see Figure 2.18, Figures 2.23–2.24, and Tables 2.2 and 2.4).

- The bridge was analyzed for HL-93 loading on three lanes of traffic using Model 3 (six members removed, A–F). The load rating passed (see Figure 2.19, Figures 2.22–2.24, and Table 2.4).

- The bridge was analyzed for an AASHTO HS20-44 load on three lanes of traffic using Model 3 (six members removed, A-F).   The load rating passed (see Figure 2.20, Figures 2.22-2.24, and Table 2.4).

- The bridge was analyzed for a permit load on one lane using Model 3 (six members removed, A–F). The structure passed this load rating (see Figure 2.21, Figures 2.22–2.24, Tables 2.2 and 2.4).

Abut. 1   Pier 2   Pier 3   Pier 4   Pier 5

Left (West) Girder

A 0.36

Left (West) Lane Truss

B 0.63

D 0.68

Center Truss

Right (East) Lane Truss

C 0.64

Right (East) Girder
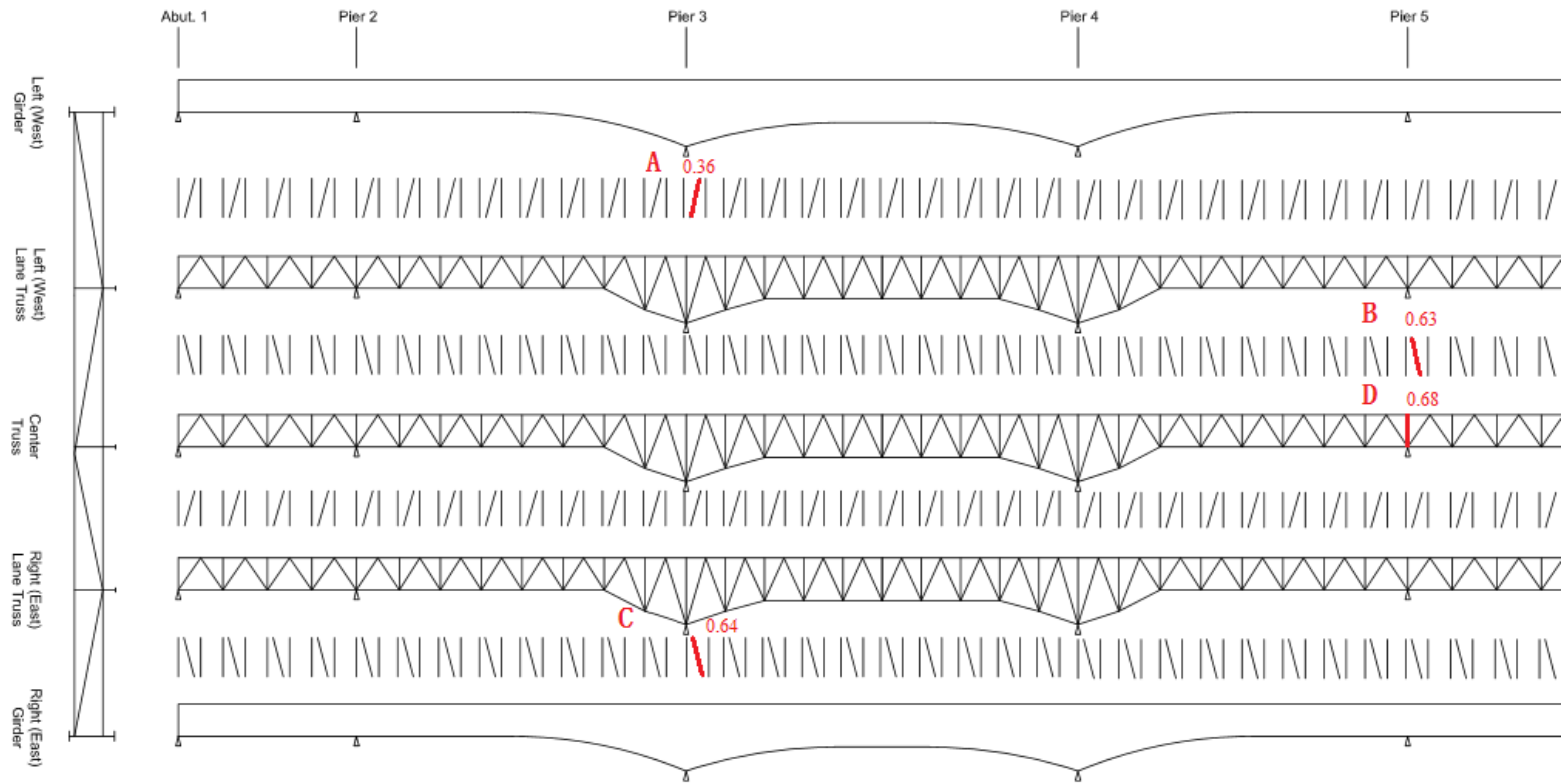
Note: All member rating factors not shown are > 1.00

LRFR HL-93 Operating Rating Factors (<1.00)

(Updated Model - As is Condition for Three Lanes)

13

Figure 2.9 Operating Load Rating: Two lanes, HL-93, as-is condition

Figure 2.10 Operating Load Rating: Two lanes, HL-93 (all rocker bearings in contact)
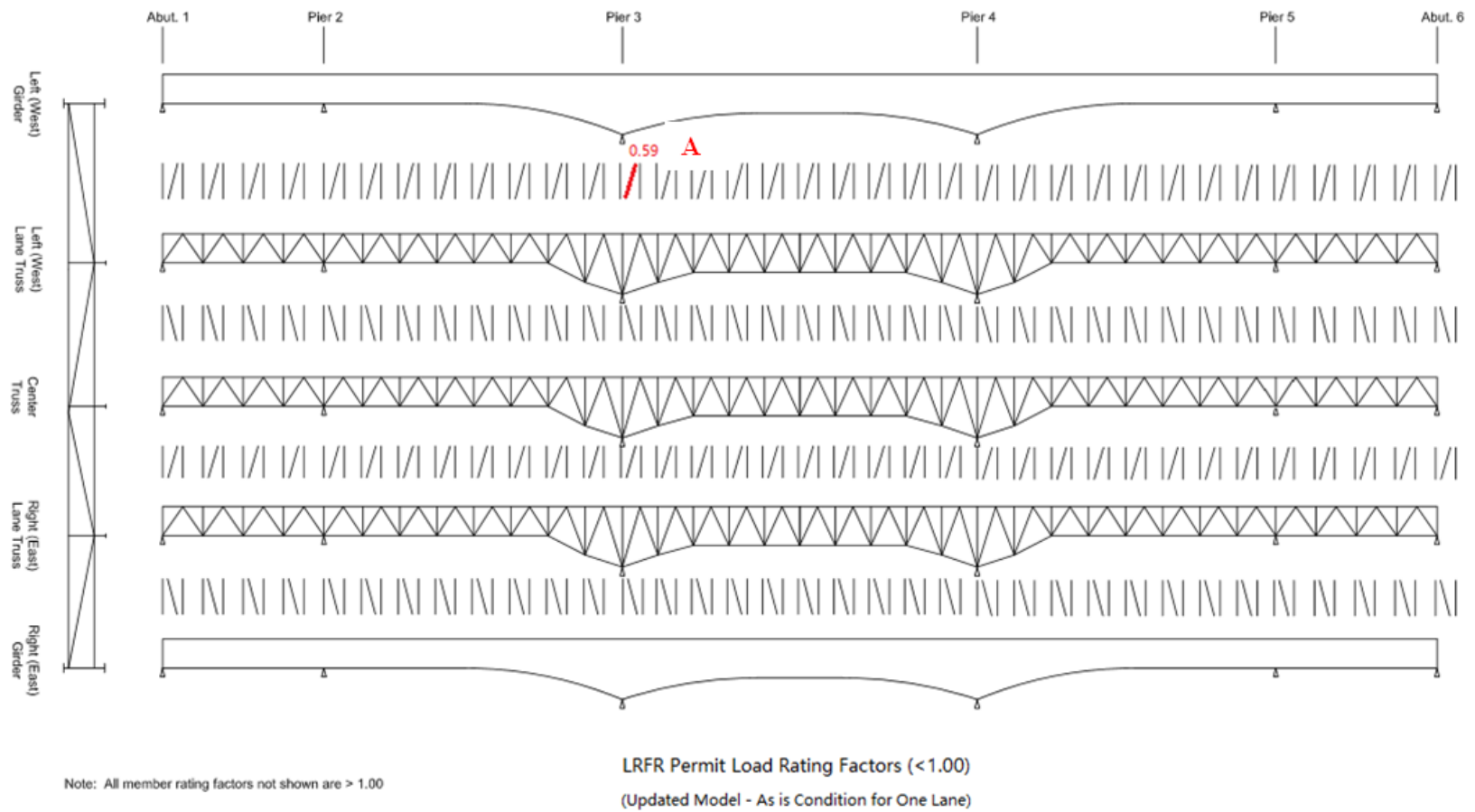
Figure 2.11 Operating Load Rating; One lane, permit load, as-is condition

L

16
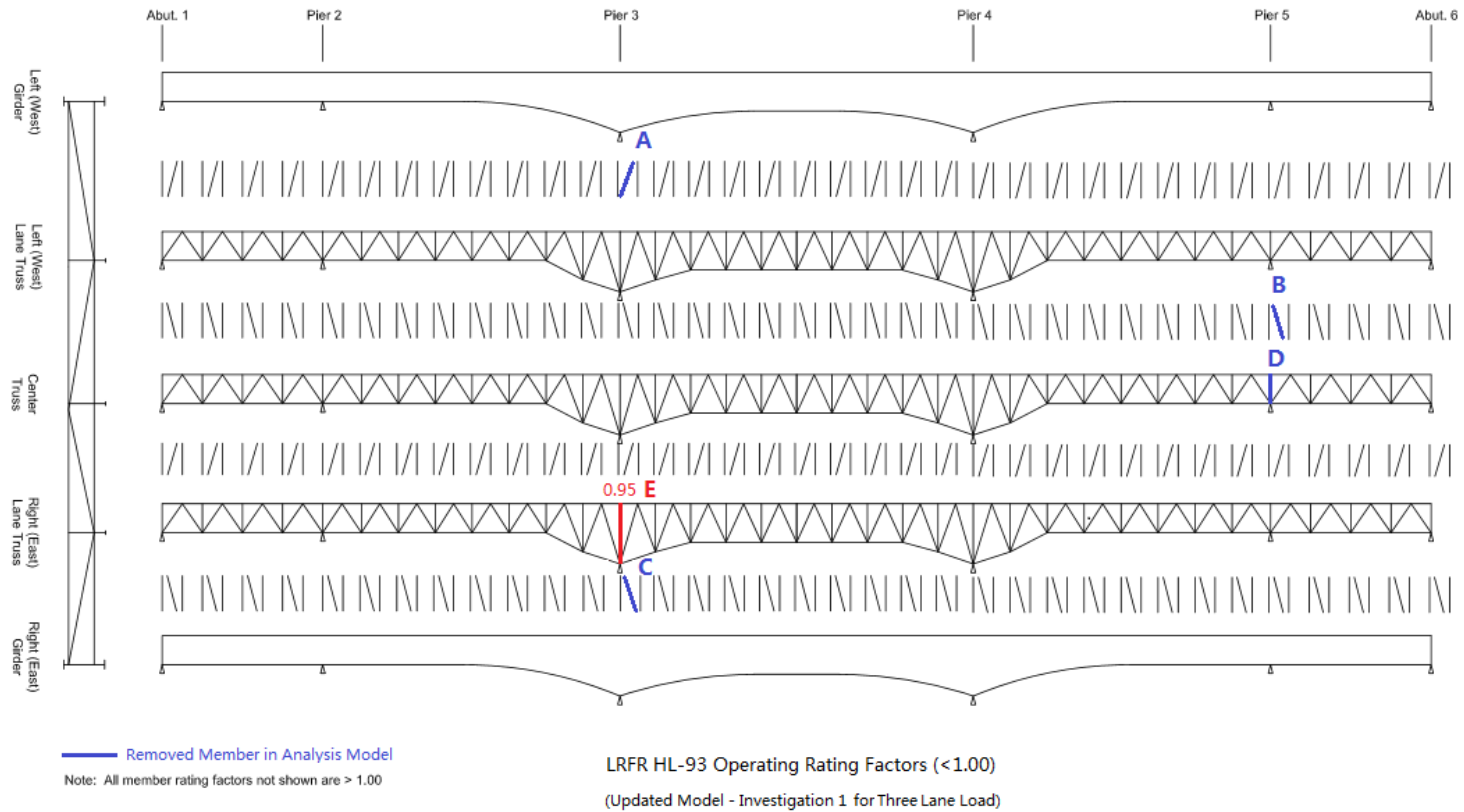
Figure 2.12 Operating Load Rating, Three lanes, HL-93, Model 1 (4 members removed)
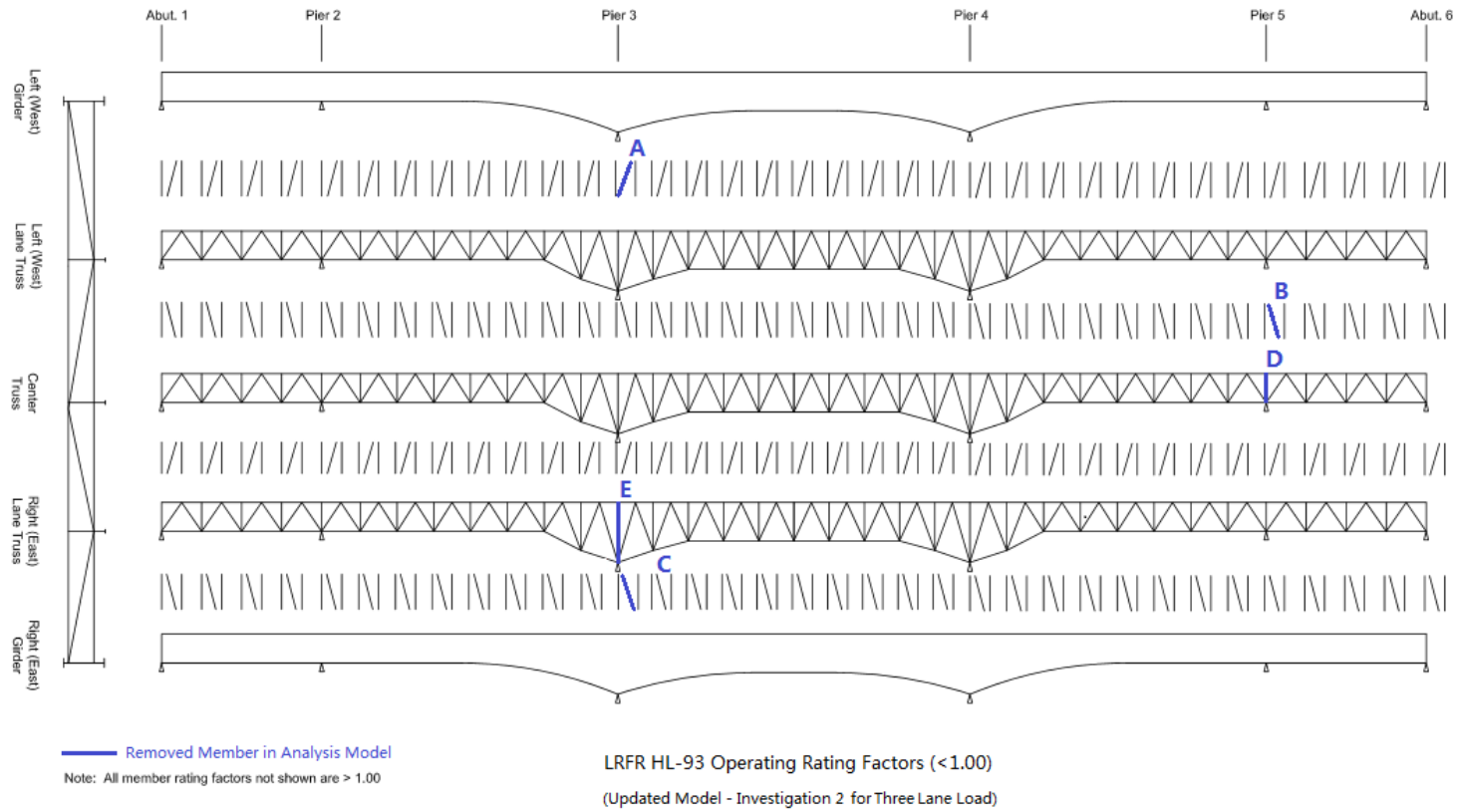
Figure 2.13 Operating Load Rating, Three lanes, HL-93, Model 2 (5 members removed)
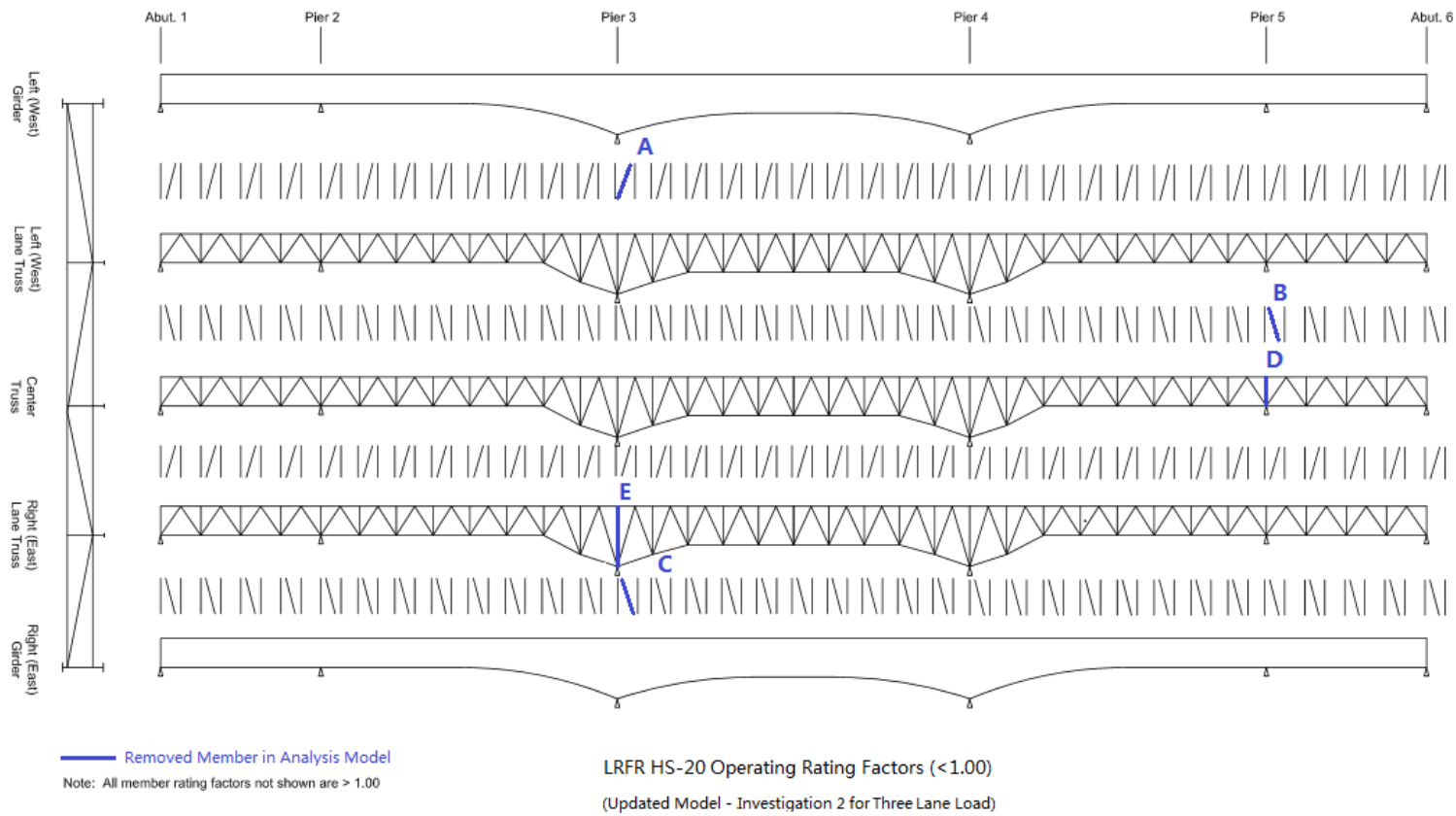
Figure 2.14 Operating Load Rating; Three lanes, HS20-44, Model 2 (5 members removed)
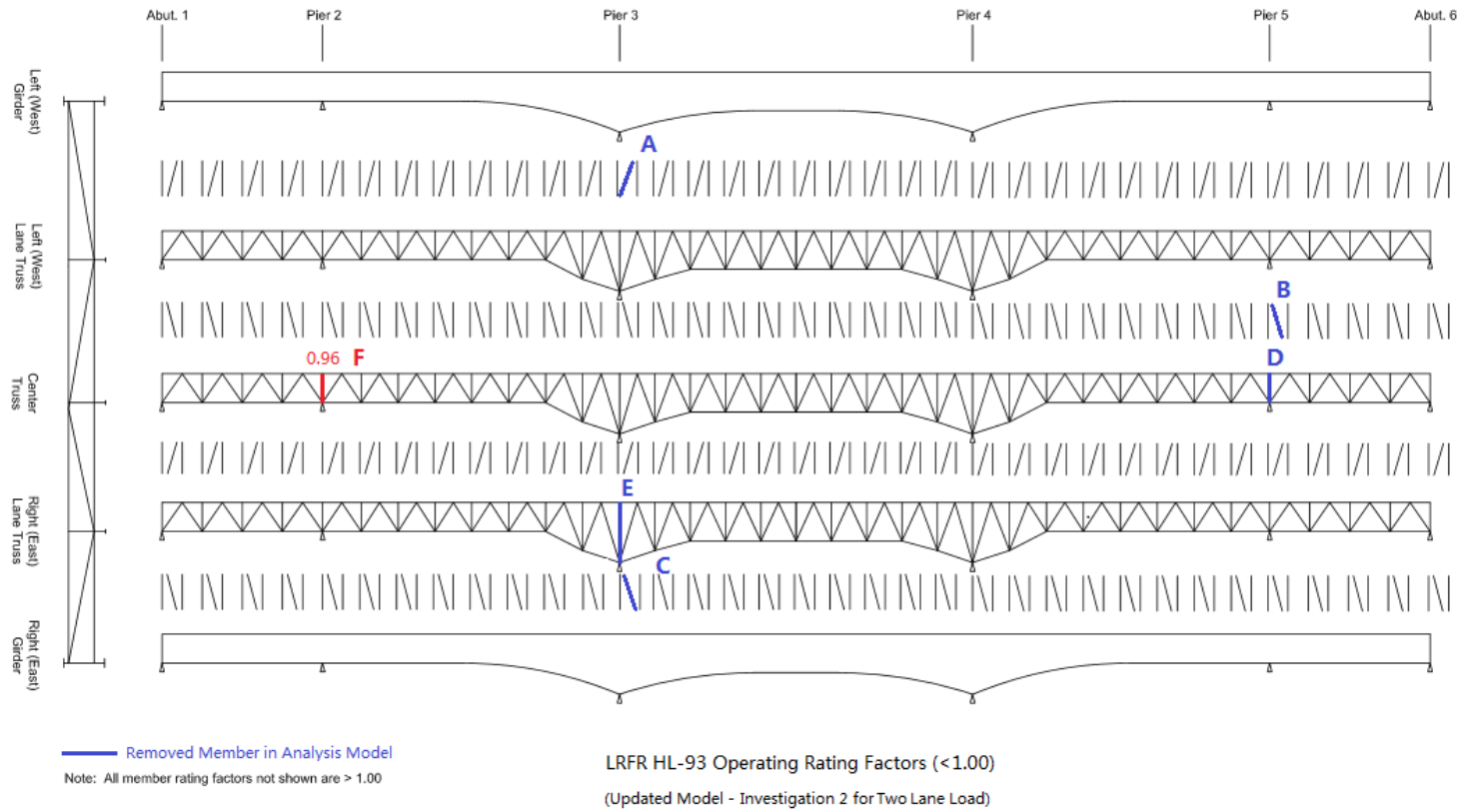
Figure 2.15 Two lanes loaded, HL-93, Model 2 (5 members removed), RF<1
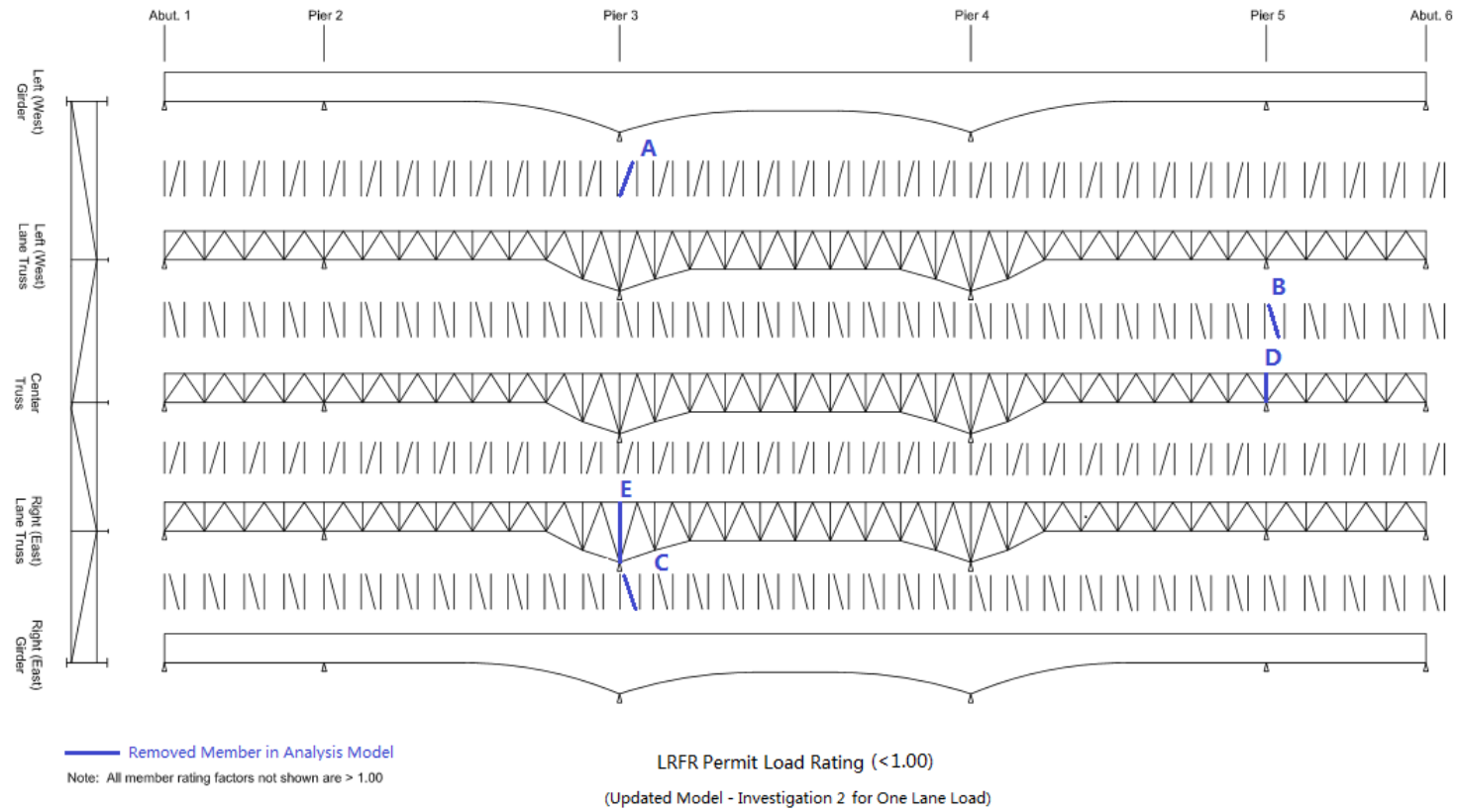
Figure 2.16 One Lane Loaded, Permit load, Model 2 (5 members removed) passed
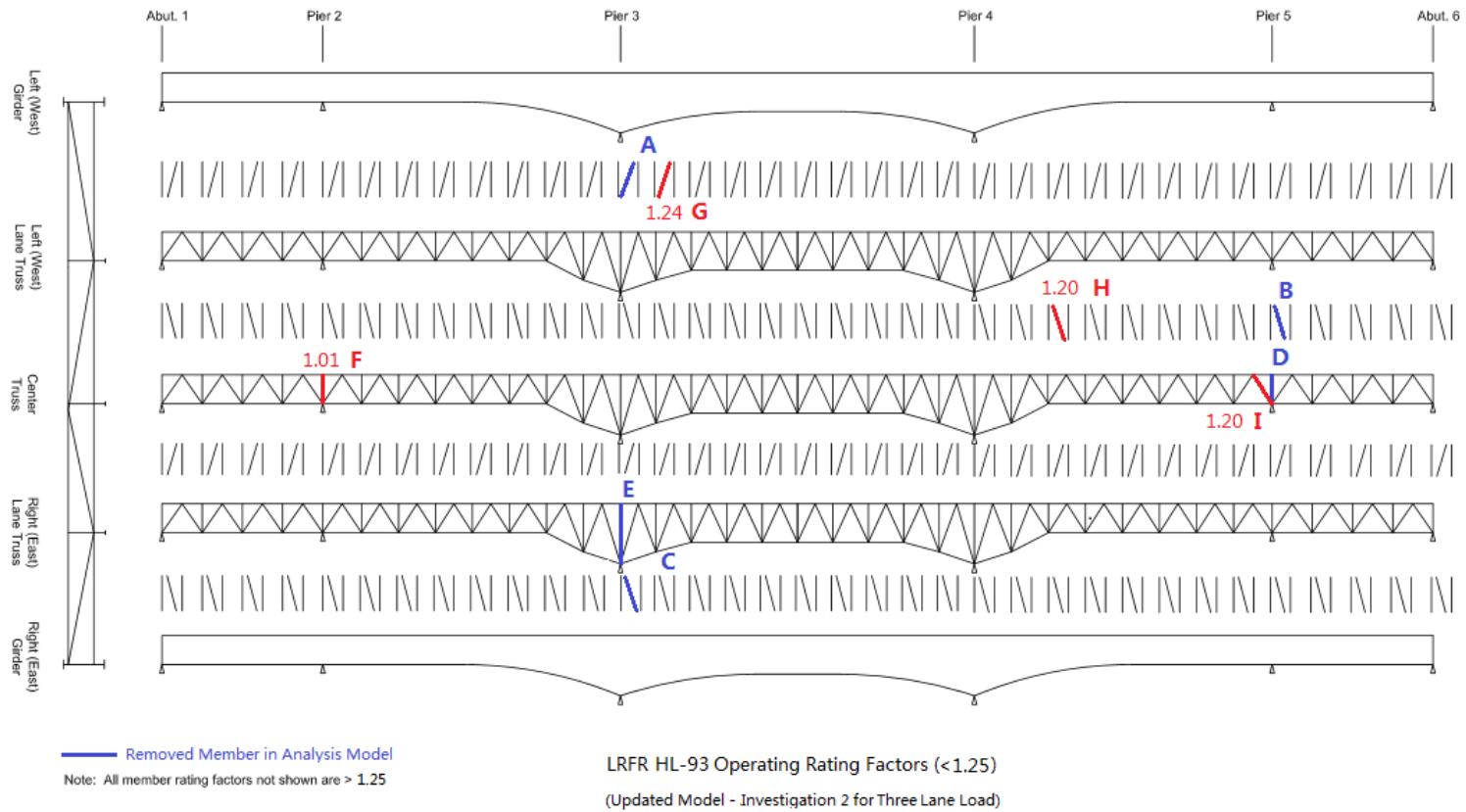
Figure 2.17 Three lanes, HL-93, Model 2 (5 members removed) results for $1 \leq RF < 1.25$
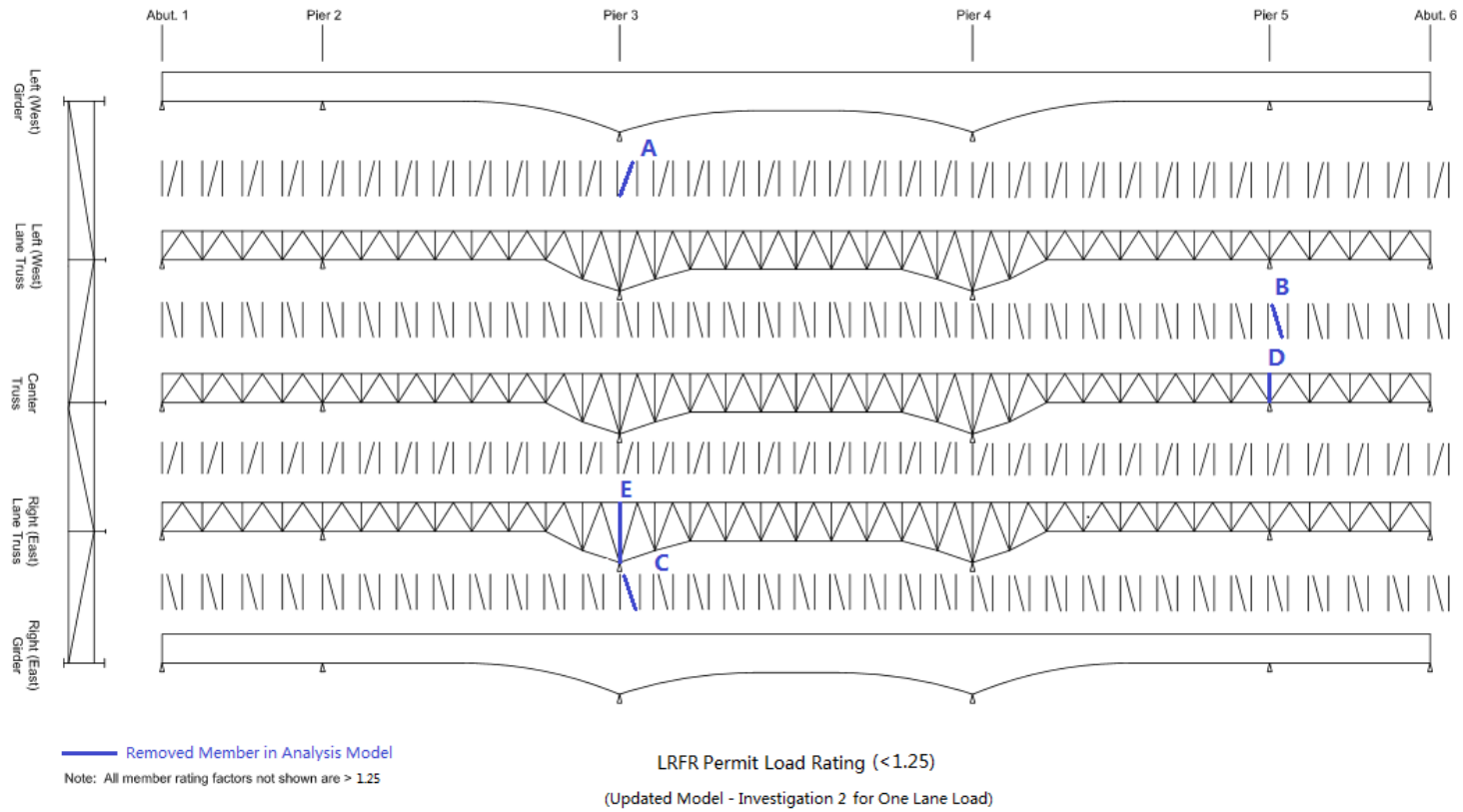
Figure 2.18 One lane, permit load, Model 2 (5 members removed) results $1 \leq RF < 1.25$
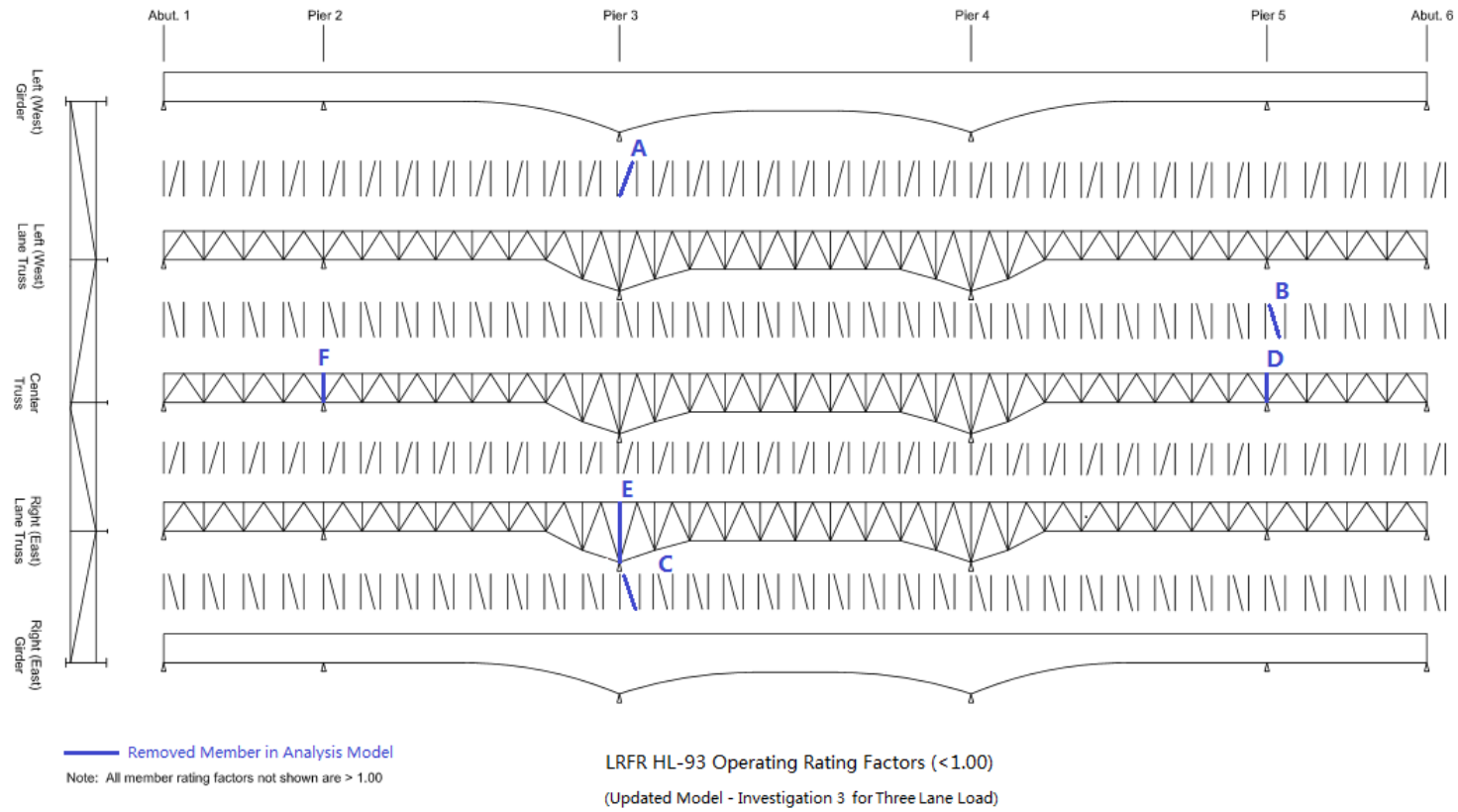
Figure 2.19 Three lanes, HL-93, Model 3 (6 members removed), load rating passed
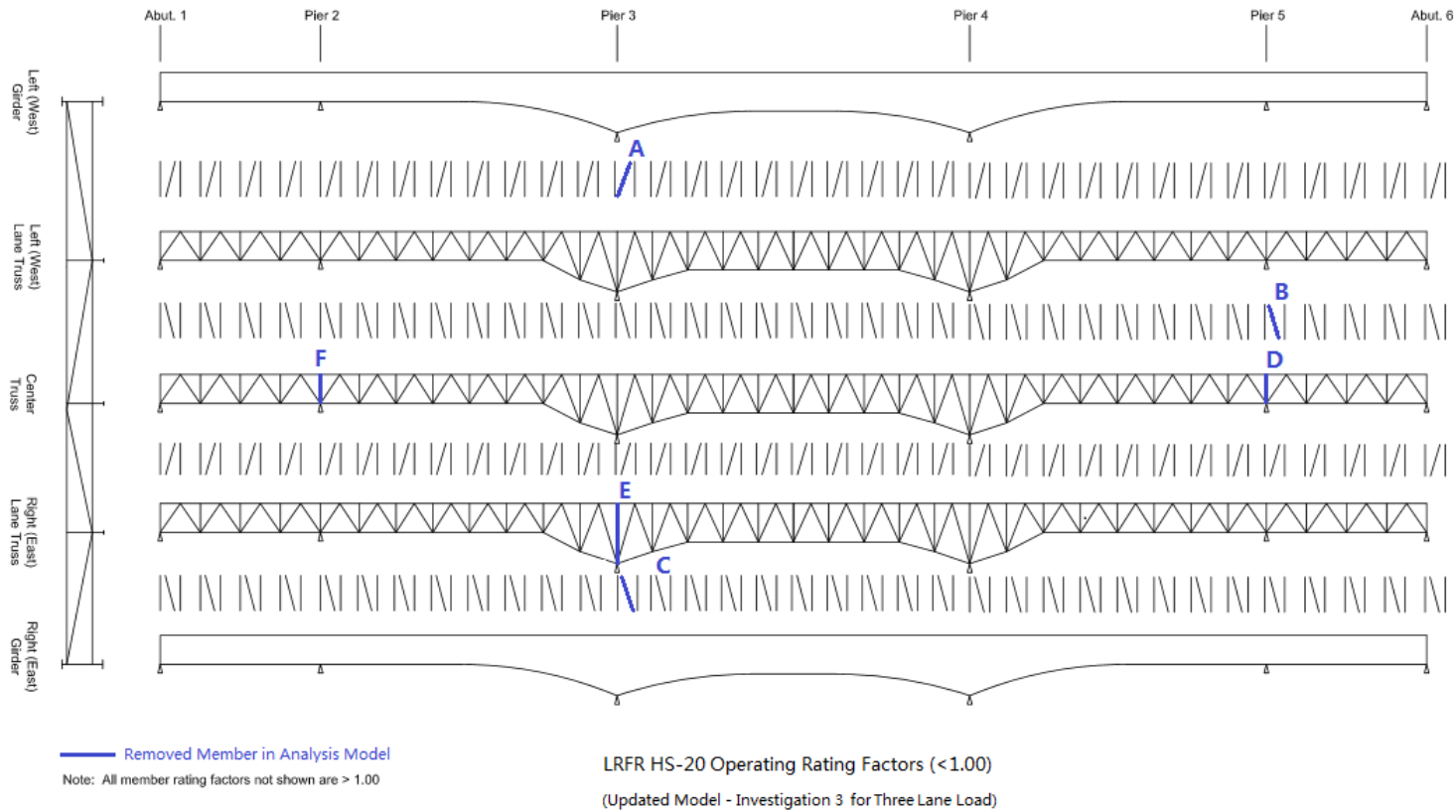
Figure 2.20 Three lanes, AASHTO 20-44, Model 3 (6 members removed), load rating passed
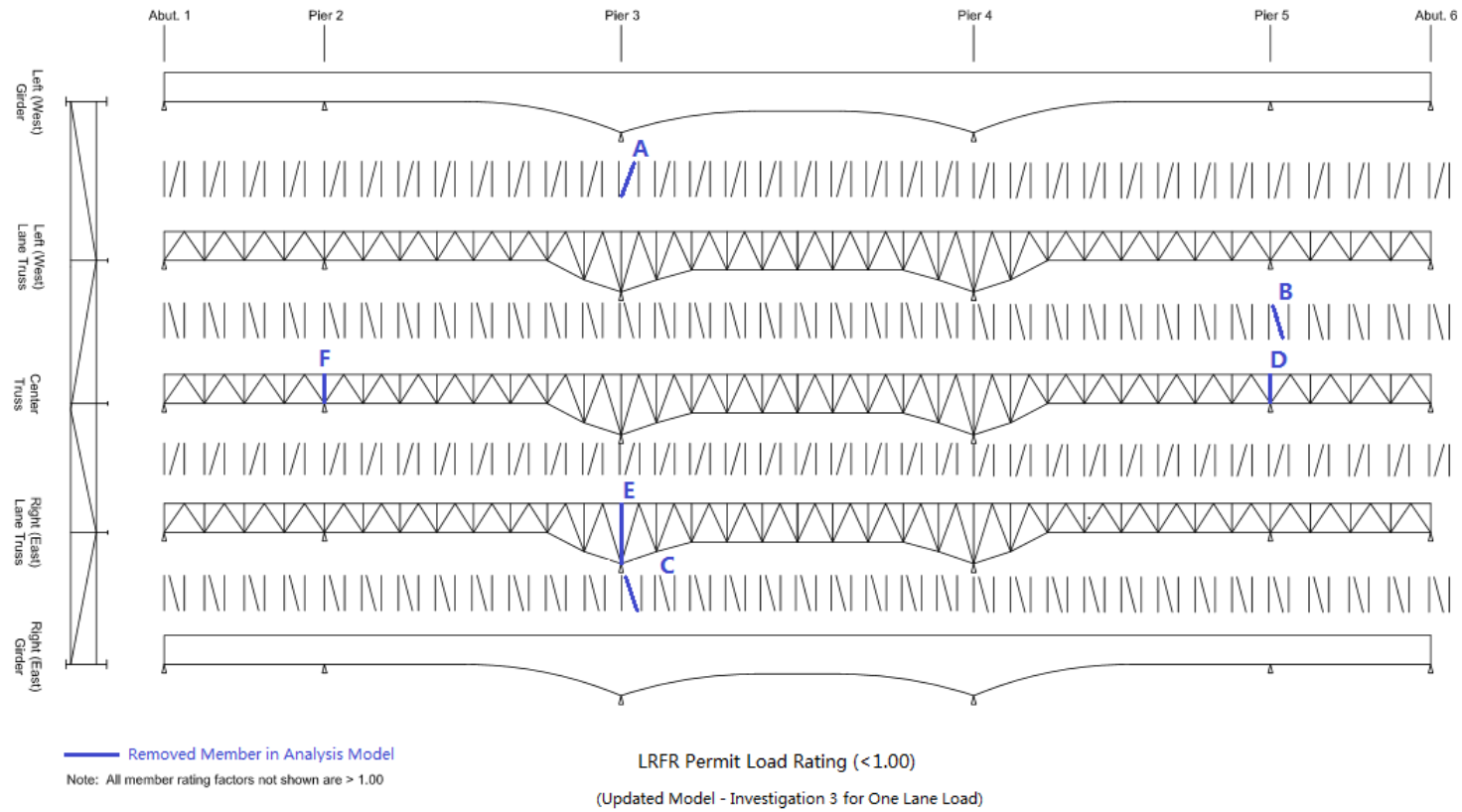
Figure 2.21 One Lane, Permit Load, Model 3 (6 members removed), load rating passed

Table 2.1 Chulitna River Bridge: A summary of member response when RF<1

Critical Locations	A	B	C	D	E	F
Member Sizes	2L6x4 ½ x 3/8	2L4x3 5/16 x 3/8	2L4x3 5/16 x 3/8	2L6x4 ½ x 3/8	2L6x4 ½ x 3/8	2L6x4 ½ x 3/8
Load Ratings:						
As-is: 3 lanes; HL-93	0.36	0.63	0.64	0.68		
As-is: 2 lanes; HL-93	0.38	0.65	0.74	0.68		
As-is: 1 lane; Permit	0.59					
Supported: 2 lanes; HL-93			0.83			
Model 1: 3 lanes; HL-93					0.95	
Model 2: 2 lanes; HL-93						0.96

Note: All other major load-carrying members had a satisfactory rating of ≥1.
"Supported" means all rocker bearings are in contact; The 5 bearings at the interior truss girders are adjusted when closed to traffic.

Table 2.2 Special permitted vehicle, axle width of 21 feet (after ADOT&PF)

Truck 1	Axle Load (kips)	16.9	28.45	28.45	34.92	34.93	33.15	33.15	31.18	31.17	30.5	30.25	32.22	32.22
	Axial Distance (ft)	0	23	5	15.5	6.08	14.5	4.42	99.75	4.42	13.5	4.4	14.42	4.42
Truck 2	Axle Load (kips)	16.8	29.025	29.025	34.725	34.725	33.025	33.025	31.75	31.75	30.825	30.825	32.6	32.6
	Axial Distance (ft)	0	23	5	15.6	6	14.6	4.5	99.9	4.5	13.3	4.5	14.6	4.5

Table 2.3 Load rating results (RF<1)

Model	As-is**	Model (1)	Model (2)	Model (2)	Model (2)	Model (2)	Model (2)	Model (3)	
Load	HL-93	HL-93	HL-93	HL-93	HS-20	HS-20	Permit Load	HL-93	
Loaded Traffic Lanes	3	3	3	2	3	2	1	3	
Member RF<1	A	E	-	F	-	-	-	-	
Cross Area (in^2)		4.49	-	4.18	-	-	-	-	
Dead Load (ksi)		-4.78	-	-6.40	-	-	-	-	
Live Load (ksi)		-6.33	-	-11.10	-	-	-	-	
Load Rating	0.36	0.95	Pass	0.96	Pass	Pass	Pass	Pass	

**Members A–D had Operating Load rating factors (RF) less than 1. The values were between 0.36 to 0.68

* Model (1) Members A, B, C, and D were removed

* Model (2) Members A, B, C, D and E were removed

* Model (3) Members A, B, C, D, E and F were removed

Table 2.4 Load rating results ($1 < RF \leq 1.25$)

FE Model	Model (2)* - 4 Secondary Members Removed				
Load	HL-93				Permit Load**
Loaded Lane	3				1
Members: $1 < RF \leq 1.25$	F	G	H	I	-
Cross Area (in^2)	4.18	9.50	4.18	19.47	-
Dead Load (ksi)	-6.40	-5.56	-1.54	-6.96	-
Live Load (ksi)	-10.58	-6.09	-5.41	-6.70	-
Load Rating	1.01	1.24	1.20	1.20	** $RF > 1.25$

Model* (2) Secondary Members A, B, C, D, and E were removed from the computer model
** All members for Permit Loads on one lane had a Load Rating greater than 1.25
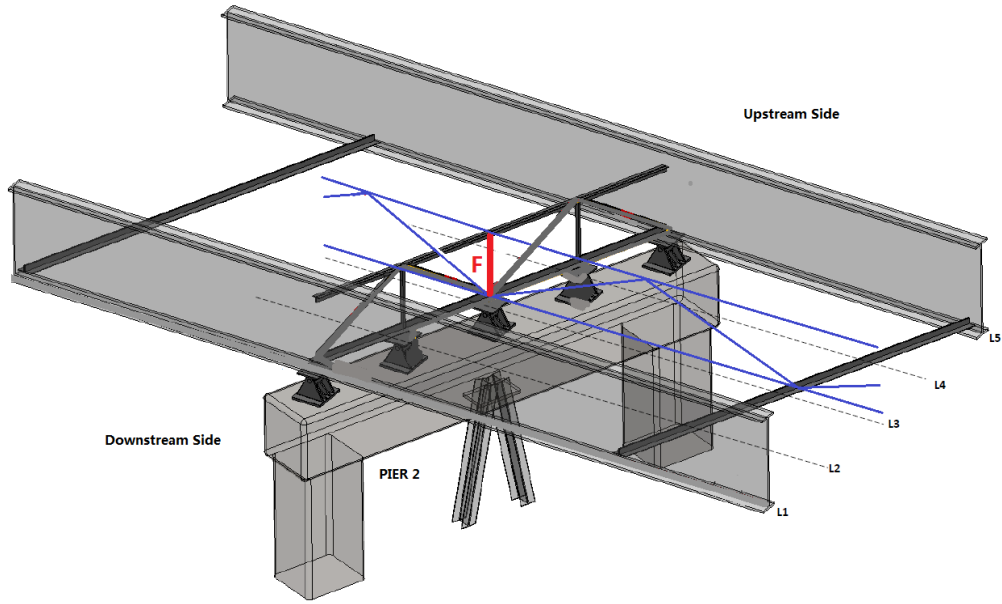
Figure 2.22 Three-dimensional view of secondary member F
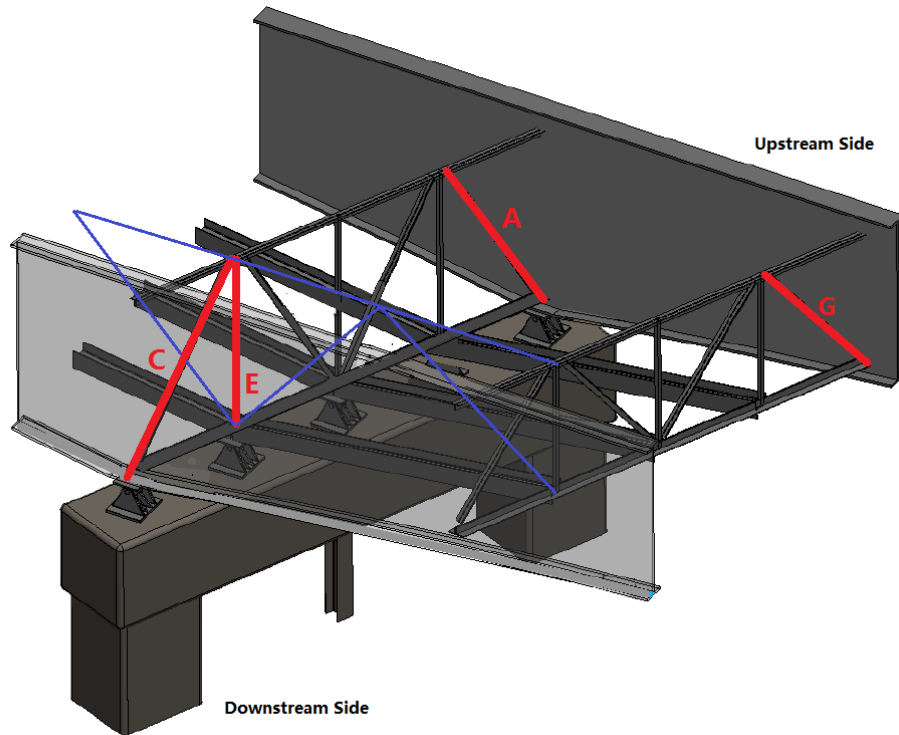
Figure 2.23 Three-dimensional view of showing members A, C, E, and G
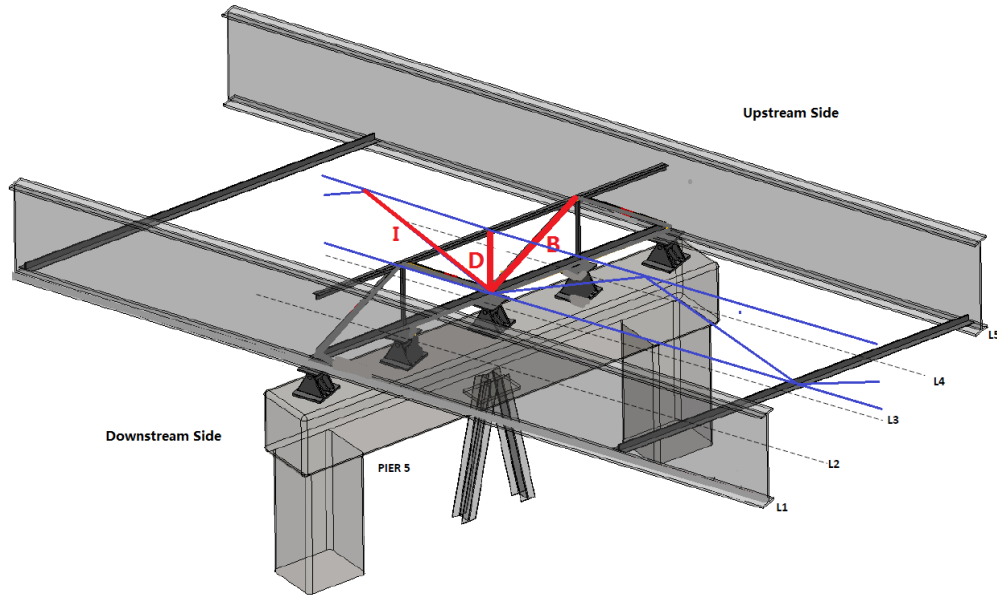
3D View at Pier 5

Figure 2.24 Three-dimensional view showing members B, D, and I
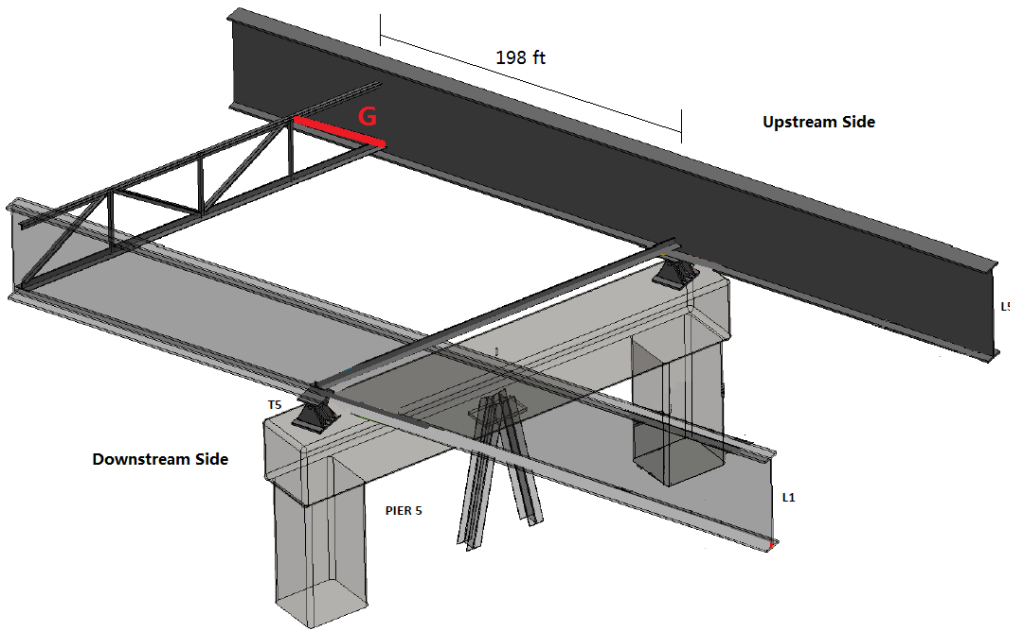
3D View at Pier 5

Figure 2.25 Three-dimensional view showing member G

Table 2.5 Summary of load ratings for bridge conditions

Load Type	Traffic Lanes	Analysis Conditions	Operating Load Rating		No. of Members with RF<1
			Member	RF	
HL-93	3	As-is	A	0.36	4
HL-93	2	As-is	A	0.38	4
HL-93	2	As-is*	D	0.83	1
Permit	1	As-is	A	0.59	1
HL-93	3	Model 1 (4 members removed)	E	0.95	1
HL-93	3	Model 2 (5 members removed)	----	Passed	none
HS20-44	3	Model 2 (5 members removed)	---	Passed	none
HL-93	2	Model 2 (5 members removed)	F	0.96	1
Permit	1	Model 2 (5 members removed)	---	Passed	none
HS20-44	3	Model 3 (6 members removed)	---	Passed	none
HL-93	3	Model 3 (6 members removed)	---	Passed	none
Permit	1	Model 3 (6 members removed)	'---	Passed	none

* All bearings were in contact in this load rating analysis.

CHAPTER 3.0 CALIBRATED FINITE ELEMENT MODEL

A simple accuracy test was conducted to refine the mesh to ensure that it converged to a reasonable estimation of the response. The simple accuracy test results showed that the original HDR finite element model (FEM) had a mesh size that would provide an acceptable level of accuracy.

Next, the FEM was calibrated against structural response, which was done by modifying elements and structural properties to more accurately describe the as-built bridge structure (see Appendices A–E). The modification process was divided into two stages: one in the longitudinal direction and the other in the transverse direction (Xiao, F., Hulsey, J. L., and Chen, G. S., 2015). Finally, the accuracy of the modified FEM was checked against structural response, as measured by the sensors at the local level (structural health monitoring system, SHMS), and the global level frequency response, as measured with 15 portable accelerometers placed on the bridge deck.

Longitudinal members such as the girder flanges, stringer flanges, composite truss lower-chord cross area, and elastic modulus of the concrete deck were selected for study to determine if these items were accurately describing the as-built bridge structure.

On September 10, 2012, three ADOT&PF dump trucks were used to load test the bridge; this was Phase 1. Static and dynamic strains, tilts, and displacements were measured for seventeen different combinations of truck positions. The measured local response data caused by these different load tests were compared with the FEM results; the differences between experimental and calculated data are the objective functions. Variables were selected and adjusted to match as-built construction drawings so that response was within a reasonable range.

The purpose was to reduce the objective functions; that is, the modeled geometry should be checked against as-built construction drawings. In addition to verifying that calculated local strains were sufficiently accurate, the calculated global (vertical, longitudinal, transverse) natural frequencies were checked against measured values (Xiao, F., Chen, G. S. and Hulsey, J. L., 2014).   This check ensured that element and material property corrections for the model would result in convergence between measured and calculated values.

In the transverse direction, the unconnected roller bearings and cross frames were selected for study. The transverse behavior was studied by evaluating load test response when two trucks were stopped at two critical cross sections. The difference between measured local

strain values and calculated values were evaluated and compared. The model was reviewed and modified to describe the as-built construction drawings. This process was continued until the model accurately described the behavior and the calculated values correlated well with the experimental values.

After model modifications, both local and global values resulted in lower errors between measured and calculated values. For local values, the largest error decreased from -512.3% to -19.9%. For global values, the largest error decreased from -10.2% to 8.9%. The modified or refined (calibrated) FEM now provides calculated values with an accuracy that is within acceptable limits for both local and global values.

CHAPTER 4.0 PROPOSED ALASKA BRIDGE MONITORING SYSTEM

4.1   General

The purpose of this chapter is to provide the reader with a clear plan for developing a structural health monitoring system (SHMS) for a bridge in the state of Alaska. Consider that it will be an objective to select the minimum number of sensors to describe bridge response to typical traffic loads, special permit loads, and exposures (snow, wind, ice forces, earthquakes, etc.)

The authors recommend evaluating bridge response by monitoring global level (macro response; i.e., acceleration ambient vibration data) and local level (micro response, such as strains and displacements at a point). In Phase 1 of these studies, the AUTC research team installed 73 sensors on the Chulitna River Bridge. The number of sensors, types, and locations were selected in collaboration with the ADOT&PF Bridge section (Hulsey, J.L., and F. Xiao. 2013). In addition, the AUTC team provided 15 temporary accelerometers for monitoring ambient vibrations (this was not part of the contract). The 73 sensors placed on the Chulitna River Bridge are presented in Table 4.1. These 73 sensors were part of the SHMS and provide local data.

Table 4.1 Summary of the SHMS sensors installed on the Chulitna River Bridge

Sensor and Locations	Number of Sensors
Rosette strain sensors	8
Strain sensors on the girders	12
Strain sensors on the composite trusses	16
Strain sensors on the concrete duck	4
Strain sensor on the diagonal members	8
Accelerometers	5
Displacement sensors	5
Temperature sensors	11
Tilter meters	4
Total	73

A total of 20 data sensors were not needed to update and calibrate the computer model. The resulting computer model was then used to load rate the bridge. The unused sensors included 8 rosettes (on the girders); 8 strain sensors (on the girders); 4 tilt meters (on the roller supports). Unused sensors are shown in Figure 4.1 by marked red circles around the sensor.

One of the issues with these systems is that data management can be overwhelming, and someone needs to be responsible for collecting and interpreting the information. Typically, warning flags should be part of the monitoring system. These flags provide the agency with a warning should a safety problem occur. If it is important to evaluate real-time data, only pertinent data should be evaluated. In this study, only 53 of the 73 were needed to evaluate the bridge response to load; see Table 4.1 for a summary of the installed sensors. Figure 4.1 show those sensors that were used to perform an evaluation of the structural response.

4.2   Selecting a SHMS for Alaska

The approach to selecting a SHMS for Alaska may look like the following:

Global: Provide a system to monitor bridge performance at the global level; this would be portable accelerometers installed at the time of the bridge inspection.

- Measure ambient accelerations at the time that a bridge inspection is performed. This can be done by using a portable system that measures accelerations. Depending on the bridge, it is recommended that 15 to 20 accelerometers be used.

Local: Install a system to monitor bridge response at the local level. The sensors should be stable without drift. The system should provide the technology to measure tilt displacements, temperatures, pressures, strains, load cells, cracks, etc. Using fiber optics is recommended as a good solution. Long-term data monitoring is often a challenge, as many bridges in Alaska are in remote areas where phone and power are not accessible. Thus, it is recommended that the multiplexer be placed on the bridge and the data monitoring system be placed off the bridge. The data monitoring system could be located off site at the office where the bridge being monitored.

- Any system that involves measuring data over a long time requires careful consideration of sensor types. For example, it is critical that the agency have a system in which the sensors do not drift over time, and the sensors must be minimally affected by stray currents from power lines, etc.

If the agency plans to study a structure for a long time, the following approach is recommended in developing a monitoring system:

a. Monitor support reactions (find live load distribution; use load cells at the bearings or support shear strain on the girders).

b. Use strain gauges to measure the behavior at critical points or at locations where there is some concern.

c. Use pressure transducers to monitor back wall-induced pressures from the embankments.

d. Use one or two accelerometers per span to monitor dynamic effects induced by traffic, earthquakes, wind, etc. This information will help in calibrating the computer model to AASHTO impact factors.

e. Install gap gauges at the top of the piers. This information will verify how the longitudinal breaking forces and other imposed horizontal forces are distributed to the structural system.

4.3   New Bridges (Proposed Monitoring Systems)

Install load cells at the bearings. This information will provide the bridge engineer with an understanding of the dead load per each support and the live load distribution for traffic and special permit loads. This approach also provides the bridge engineer with an understanding of load paths. A minimum number of additional sensors can be added to address possible changes in load paths within the structural framing system. This information will inform the engineer of the change in health of the structure. It is suggested that the agency measure the ambient vibrational response (global data) every two years when the bridge is inspected.

4.4   Existing Bridges (Proposed Monitoring Systems)

If the agency is planning to monitor an existing bridge, built-in dead load stresses are not known; however, live load distribution can be accurately monitored by providing sensors at members that frame into the support bearings. It is suggested that the agency measure the ambient vibrational response (global data) every two years when the bridge is being inspected.

4.5   All Bridges (Proposed Monitoring Systems)

Install strain gauges at critical points in the structure or at locations of concern. At the time the bridge is inspected, it is recommended that the agency monitor the natural frequency of the structure. This may be accomplished by placing between 15 and 20 portable accelerometers along the bridge centerline. As part of this effort, the agency should consider measuring the

ambient vibrational response in the transverse, longitudinal, and vertical directions. This effort is quick, and the equipment can be part of the bridge inspection program.
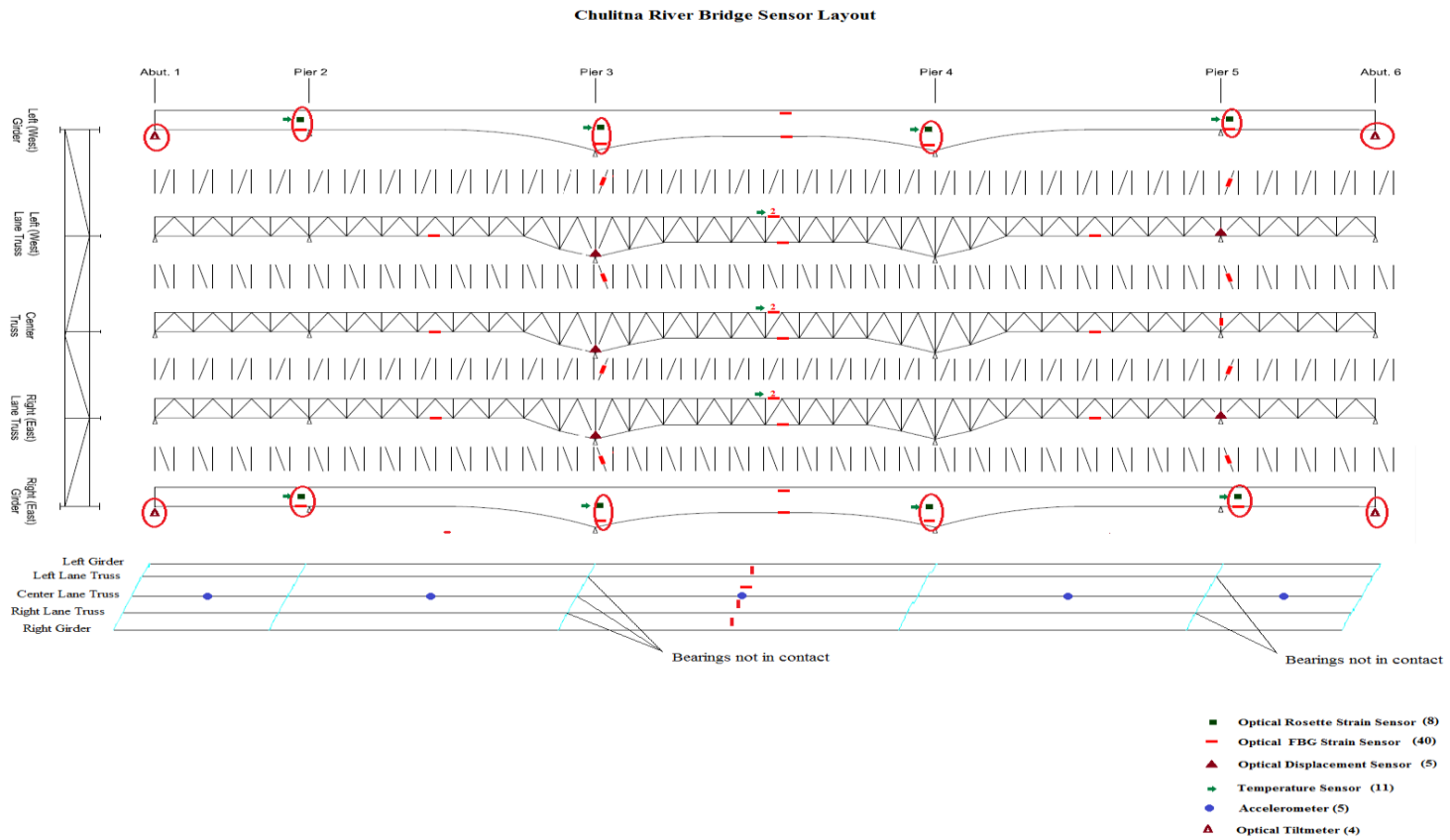
Figure 4.1 Sensors used for evaluating the bridge response

CHAPTER 5.0 CONCLUSIONS

The purpose of this research on the Chulitna River Bridge was (1) to develop a finite element tool that could properly assess the bridge for 1993 AASHTO Load Resistance Factor Design (LRFD) bridge loads and special permit loads, and (2) to evaluate the level of stress that was being introduced into the bridge by truck traffic and special permit loads. In addition to studying the bridge's response to traffic, the researchers examined the stress level caused by live loads. The history of how structural modifications were conducted to widen this bridge in 1993 was not found. Thus, the magnitude of the induced dead load stresses is not known.

5.1   Phase 1 (Previous Study)

Selection and installation of a structural health monitoring system (SHMS) occurred during Phase 1. In spring 2012, the AUTC research team selected a SHMS. This system uses fiber-optic sensors. The fiber-optic sensors were selected because of the long-term stability of this type of instrumentation. The research team then took a week-long course in theory, application, and installation of available fiber-optic sensor technology. Training was provided on both theory and techniques for field installations and fiber splicing. Prior to sensor installation, the bridge was analyzed for AASHTO loads, and sensors were selected to assist in evaluating bridge health and to assist the research team in determining critical members. In late summer, Chandler Monitoring Systems (CMS) and the AUTC research team installed the SHMS.

5.1.1 Gravity load testing

On September 9, 2012, test trucks were measured and weighed. CMS calibrated the system, and the AUTC research team laid out the test plan for the following day. On September 10, 2012, the bridge was load-tested with seventeen different static and dynamic load combinations of three heavily loaded dump trucks (two bellies and a side dump) (Hulsey and Xiao, 2013; Hulsey et al., 2012a, 2012b).

In all cases, the bridge was loaded using ADOT&PF dump trucks (two belly and one side dump). On September 9, 2012, the trucks were weighed and measured. During testing, static tests were performed by directing the drivers to position the front axles over a given location that was painted on the bridge deck prior to testing. Once wheels were in position, the trucks stopped, and the bridge allowed to quiet down, data were recorded.

Both static and dynamic tests were performed using three dump trucks (two belly dumps and a side dump). Information on the test trucks is presented in Appendix F.

5.1.2 *Ambient testing (2012 tests were Phase 1; 2013 tests were Phase 2)*

In addition to subjecting the bridge to truck loads, ambient vibration tests were also conducted in August 2012 and again in the summer of 2013. These tests are inexpensive and quick to conduct. For these tests, the bridge is excited, and vibrational response (frequency) is monitored at 15 different accelerometers along the bridge centerline. The test conducted in August 2012 provides a baseline describing the health of this structure (Xiao, F., Chen, G. S. and Hulsey, J. L., (2014).

5.2 Phase 2 (Current Study)

During Phase 2 of the study, SHMS local data were recorded between the end of September 2012 and December 31, 2013. System monitoring occurred remotely, in that the sensors could be monitored in real time from the office of one of the researchers at the University of Alaska Fairbanks campus.

In addition to monitoring traffic loads, an ambient vibration test was conducted during the summer 2012. This test was done by setting up 15 accelerometers along the bridge centerline and digitally recording global vibration data for longitudinal, transverse, and vertical excitations. The second ambient vibration test was conducted during summer 2013. This test provided a determination of possible change in the bridge over that one-year period (like going to the doctor for a physical exam).

The finite element model (FEM) was calibrated to as-built conditions. Using the calibrated FEM, the program was used to evaluate predicted HL-93 live load stresses. Comparisons between FEM calculated strain data and the local (SHMS) experimental data were made for the seventeen different September 10, 2012, load cases. The model was calibrated to measured global frequencies for this bridge. These data were recorded at two different times: August 2012 and May 2013. The calibrated finite model provides very good results for both local and global data. Based on these findings, the FEM could be confidently used to predict the behavior of the Chulitna River Bridge. Our findings show that member live load stresses for the bridge are low. Dead load stresses for the interior truss girder are high, but not defined. The study had three conclusive outcomes:

5.2.1 Outcome 1 – Finite element model

A finite element model is now available. It is calibrated against two different data sets: measured ambient frequencies (global data) and SHMS (local strain) data. The results are satisfactory, and the model can be reliably used to evaluate bridge response such as HL-93 AASHTO loads and special permit loads that will be traveling across the Chulitna River Bridge.

5.2.2 Outcome 2 – Structural evaluation and load rating

The bridge was load-rated for two different conditions: One is the existing condition and the other is based on modifying the bridge so that load is carried by all the support bearings. Between one and four members did not pass the required bridge load rating of ≥ 1. These are secondary members and are on the lower section of the interior truss girder near the bearing supports that are not in contact with the superstructure (see Chapter 2). The bridge was also load rated by removing up to six secondary members. The results are presented below in Table 5.1 and the details are given in Chapter 2.

Table 5.1 Summary of load ratings for bridge conditions

Load Type	Traffic Lanes	Analysis Conditions	Operating Load Rating		No. of Members with RF<1
			Member	RF	
HS20-44	3	Model 3(6 members removed)	---	Passed	none
HL-93	3	Model 3 (6 members removed)	---	Passed	none
Permit	1	Model 3 (6 members removed)	'---	Passed	none

* All bearings were in contact in this load rating analysis.

5.2.3 Outcome 3 – LRFR HL-93 live load stresses for the critical members

Member stresses in three of the four interior truss girder members near the bearing supports not in contact with the superstructure have calculated dead load stresses that were around 50% of member capacity. If the gap (separation) between the five bearing supports and the superstructure occurred during construction widening and strengthening, there is low probability that the stresses in these members are this high. Depending on the construction sequence, it is likely that the exterior girders picked up most of the dead load. Although the construction sequence information requested was not found, it is possible that the answer to how

construction widening occurred may be somewhere else within the ADOT&PF archives and should be further investigated.

REFERENCES

AASHTO. 2011. *Manual for Bridge Evaluation*, 2nd Edition, with 2011 Interim Specifications, American Association of State Highway and Transportation Officals, ISBN 1-56051-496-1.

AASHTO. 2012. *LRFD Bridge Design Specifications, Customary U.S. Units.* American Association of State Highway and Transportation Officals, ISBN 978-1-56051-523-4, Publication Code: LRFDIS-6.

CSiBridge 2014. "Integrated 3-D Bridge Analysis, Design, Design and Rating." Computers and Structures, Inc., Walnut Creek, CA 94596, USA.

Hulsey, J.L., P. Brandon, and F. Xiao. 2012a. "Structural Health Monitoring and Condition Assessment of Chulitna River Bridge: Sensor Selection and Field Installation Report." Alaska Department of Transportation Research, Development, and Technology Transfer, Fairbanks, Alaska.

Hulsey, J.L., P. Brandon, and F. Xiao. 2012b. "Structural Health Monitoring and Condition Assessment of Chulitna River Bridge: Load Test Report." Alaska Department of Transportation Research, Development, and Technology Transfer, Fairbanks, Alaska.

Hulsey, J. L., Xiao, F., and Chen, G. S., (2013), Structural Health Monitoring System Optimization For A Bridge, 6TH International Conference on Structural Health Monitoring of Intelligent Infrastructure, Dec.9, Hong Kong, China.

SAP2000 Ver. 14, 2014. "Integrated 3-D Bridge Analysis, Design, Design and Rating. Computers and Structures, Inc., Walnut Creek, CA 94596, USA.

Steel Bridge Design Handbook, 2012, Load Rating of Steel Bridges, Publication No. FHWA-IF-12-052 - Vol. 18, November.

Xiao, F., Chen, G. S. and Hulsey, J. L., (2014), Experimental Investigation of a Bridge under Traffic Loadings, Advanced Materials Research, Vols. 875-877, 1989-1993, Trans Tech Publication.

Xiao, F., Hulsey, J. L., and Chen, G. S., (2015), Multi-direction Bridge Model Updating using Static and Dynamic Measurement, Applied Physics Research, Vol. 7, No. 1.

APPENDIX A – SIMPLE ACCURACY TEST

Before model changes were made, simple accuracy tests were performed to calibrate a three-dimensional SAAP2000 finite element model of the Chulitna River Bridge. This model was provided by HDR (2011) and it provided the baseline for model refinement. That is, the number of elements (original mesh) was increased in an effort to evaluate the results for a newly refined mesh. This test was conducted to ensure that it would converge to provide a reasonable estimate of the structural response. The desired level of accuracy was set at 2%. Subsequently, the mesh size was reduced to half its current size to determine if the resulting displacements and forces would change significantly or if the change was small enough to be considered acceptable. Multiple locations on the bridge were checked. These locations were ones of critical interest to the project (i.e., high tension, large displacement, etc.). Nine sections were considered when checking the strains and stresses. These nine sections are located in different spans and sides of the bridge. Four longitudinal displacements on different sides of the abutments were selected for checking. The FEM mesh size was reduced to half its current size in both lines and areas. In Table A.1, the error shows the difference between the original FEM model and the refined model. Comparison is based on three trucks that were stopped and positioned so that the front axles were 369 feet from the south abutment (Abutment 1); the three trucks were in the middle of Span 3.

The locations that are presented in Table A.1 are illustrated in Figure A.1. Table A.1 indicates that the error between the two models is low. Ignoring the sign, the largest error is 1.04%, which is within the acceptable the level of accuracy. In general, the fine mesh used in the original HDR model should give sufficiently accurate results.

At this point, the results of this test simply prove that if this model represents the actual bridge structure, the model will provide sufficiently accurate strains, displacements, and forces for a given set of loads. The results of this test do not prove that the model represents the bridge structure that is being studied.

Table A.1 Simple accuracy comparison between the HDR model and the refined model

	Locations		Number	HDR Model	Refined Model	Error (%)
Force (lb)	Mid-Span 2 Lower Chord	Downstream Side	1	-25,388	-25,476	-0.35
		Middle	2	-25,739	-25,858	-0.46
		Upstream Side	3	-26,612	-26,673	-0.23
	Mid-Span 3 Lower Chord	Downstream Side	4	80,867	81,199	-0.41
		Middle	5	83,554	83,893	-0.41
		Upstream Side	6	81,238	81,584	-0.43
	Mid-Span 4 Lower Chord	Downstream Side	7	-26,447	-26,562	-0.43
		Middle	8	-25,474	-25,624	-0.59
		Upstream Side	9	-25,546	-25,625	-0.31
Displacement Long. Dir. (mm)	Abutment 1 Roller Support	Downstream Side	10	-2.81	-2.84	-1.04
		Upstream Side	11	-2.82	-2.84	-0.66
	Abutment 2 Roller Support	Downstream Side	12	-2.21	-2.23	-0.92
		Upstream Side	13	-2.21	-2.21	-0.12
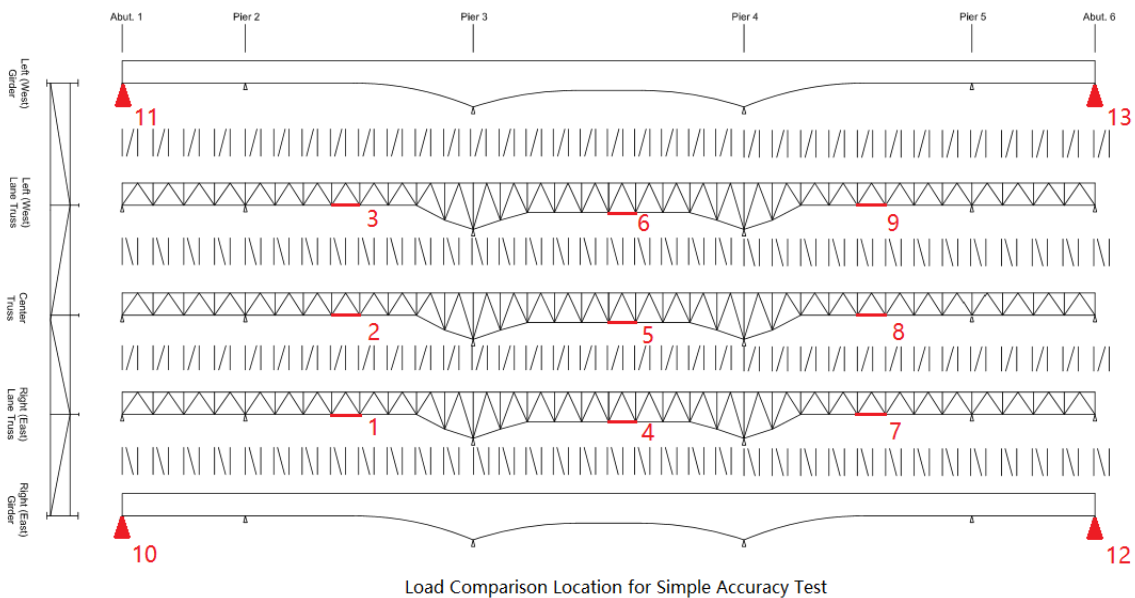
Figure A.1 Locations where the influence of mesh refinement was checked (see Table A.1).

APPENDIX A – REFERENCES

HDR, Inc., 2011, "Load Rating and Structural Assessment Load Rating Report", Bridge No. 255: Chulitna River Bridge".

APPENDIX B – LONGITUDINAL BEHAVIOR TEST

Thirteen fiber-optic strain sensors were installed in Phase 1 at the middle of Span 3 (Hulsey et al., 2012a). The strains in these sensors were used to evaluate the influence of the three ADOT&PF trucks driving side by side (Hulsey et al., 2012b).

Figures B.1, B.2, and B.3 show a comparison between stresses obtained from measured strain data and the "before modification" HDR FEM calculated mid-span stresses. Results indicate that the FEM-calculated stresses carried by the composite trusses are higher than measured; that is, calculated lower chord stresses are higher than measured (Hulsey and Xiao, 2013). This finding illustrates that the FEM does not properly represent the distribution of stiffness between the bridge composite stringers and the girders. In consideration of these problems, 14 objective functions (variables) were selected for study. Modifications to the objective functions affected load distribution for the composite trusses and girders.
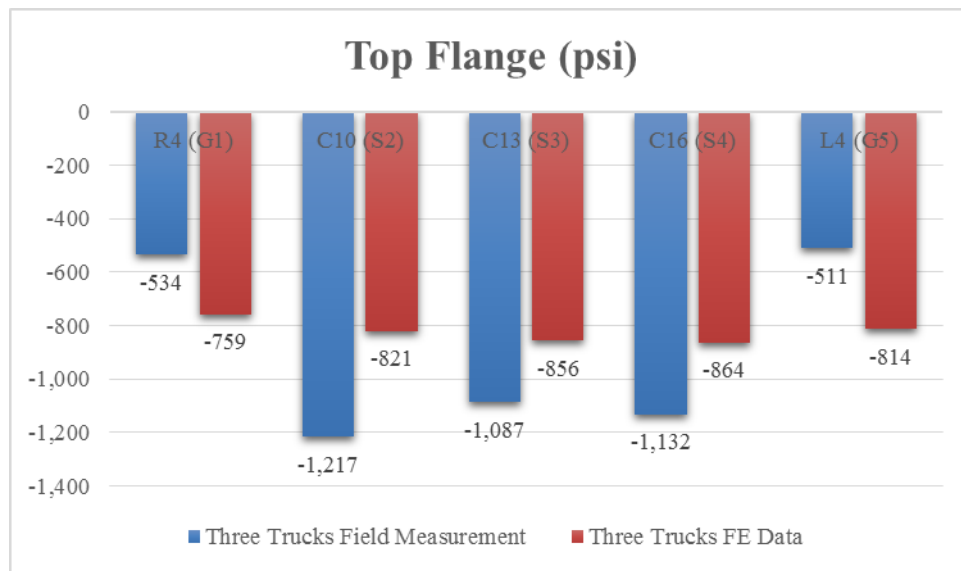
Figure B.1 Top flange stress comparison between field measured and calculated values (psi)
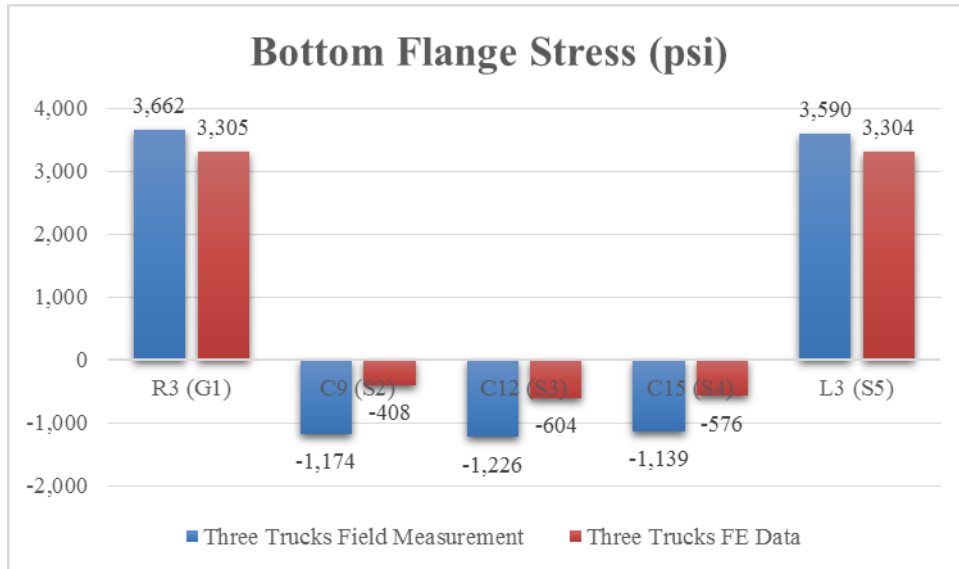
Figure B.2 Bottom flange stress comparison between measured and calculated values (psi)
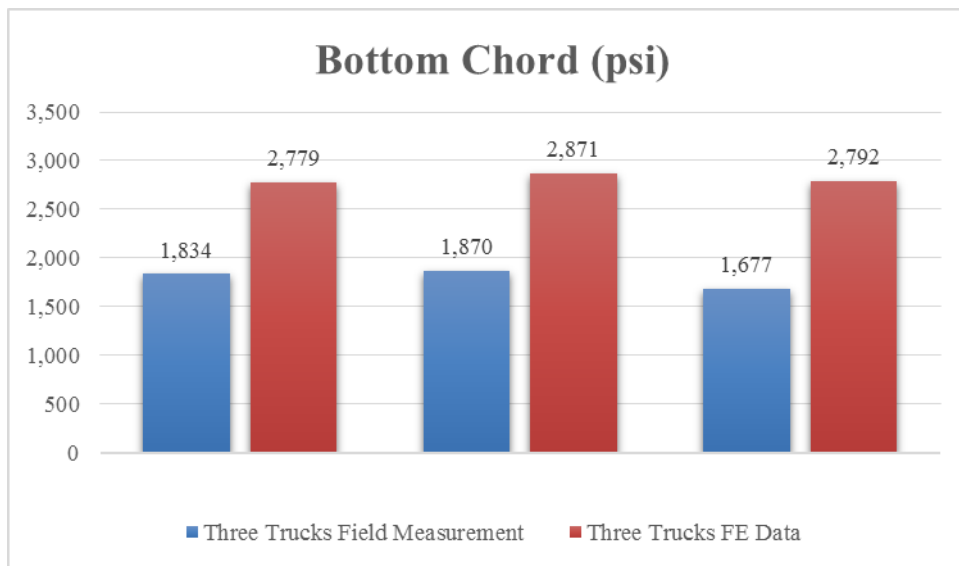
Figure B.3 Lower chord stress comparison between measured and calculated values (psi)

APPENDIX B – REFERENCES

Hulsey, J.L., P. Brandon, and F. Xiao. 2012a. "Structural Health Monitoring and Condition Assessment of Chulitna River Bridge: Sensor Selection and Field Installation Report." Alaska Department of Transportation Research, Development, and Technology Transfer, Fairbanks, Alaska.

Hulsey, J.L., P. Brandon, and F. Xiao. 2012b. "Structural Health Monitoring and Condition Assessment of Chulitna River Bridge: Load Test Report." Alaska Department of Transportation Research, Development, and Technology Transfer, Fairbanks, Alaska.

Hulsey, J.L., and F. Xiao. 2013. "Mid-span Loading Report." Alaska Department of Transportation Research, Development, and Technology Transfer, Fairbanks, Alaska.

APPENDIX C – MODEL IMPROVEMENTS (LONGITUDINAL DIRECTION)

Initially, members likely to affect structural response the most were identified. In selecting objective functions for study, member sectional data and member geometry were selected to better reflect 1993 as-built construction. According to the longitudinal behavior described by the unmodified HDR FEM, the largest error exists in a lower chord member. Modifications showed that if the cross-sectional area in the lower chord was reduced to 0.43, the resulting error in local strain dropped below 50%. This modification resulted in a change in behavior, and the largest error between measured and calculated stresses was now in the composite truss lower flange. Bridge response was investigated to a change in stiffness for the concrete deck. Changing the elastic modulus of the concrete deck to 3,000 ksi improved structural response, and the error between the calculated and measured stresses were reduced to 5%. However, the difference between the global experimental frequency response and calculated values caused the percent error to increase to 15% (that is, the stiffness change went from too stiff to too flexible). In order to balance the difference in error between local and global values, the elastic modulus of the concrete deck was changed to 3,300 ksi and the stringer lower flange area was changed from 2.0 to 2.5. The change in area represents the actual area shown on the as-built construction drawings. Table C.1 shows the influence of these modifications on structural response. Tables C.2, C.3, and C.4 show the longitudinal difference between experimental and calculated stresses for both global and local values.

Ignoring signs, the largest error for the global values decreased from -10.2% to 8.8%, and the largest error for the local values decreased from -66.4% to -17.8% in the longitudinal direction. The global measured data are from an ambient test, and the local data are based on the 13 fiber-optic strain sensors near the middle of Span 3.

Table C.1 FEM using revised variables

Bridge Sections	Locations	Property Modifiers	
Composite Trusses	3 Lower Chord	Area	0.43
Girders	2 Top Flange	Area	0.54
	2 Bottom Flange	Area	0.85
Stringer	3 Top Flange	Area	1.24
	2 Bottom Flange (No. 2,4)	Area	2.0
	Bottom Flange (No. 3)	Area	2.5
Concrete Deck	Throughout the deck	Elastic Modulus (ksi)	3,300

Table C.2 Natural frequency differences after model revisions for longitudinal behavior

Mode	Field Measurement (Hz)	Long. Updated FEM (Hz)	Difference (%)
Longitudinal Mode 1	1.500	1.368	8.8
Longitudinal Mode 2	2.190	2.036	7.0
Vertical Mode 1	2.846	2.773	2.6
Vertical Mode 2	3.224	3.196	0.9
Vertical Mode 3	4.580	4.271	6.8
Transverse Mode 1	2.095	2.168	-3.5
Transverse Mode 2	2.346	2.325	0.9
Transverse Mode 3	2.782	2.683	3.6

Table C.3 Difference in flange stress (%) after model revisions for longitudinal behavior

Load Case	Location	1	2	3	4	5
	Sensor Number	R3	C9	C12	C15	L3
Top Flange	Field Measurement	-12.4	-12.0	--17.8	-17.4	-12.0
	Updated FE Data					
Bottom Flange	Field Measurement	-6.7	1.2	11.7	5.7	-9.9
	FE Data					

Table C.4 Difference in lower chord stress (%) after model revisions for longitudinal behavior

Load Case	Location	1	2	3
	Sensor Number	R3	C9	C12
Top Flange	Field Measurement	-3.8	-6.8	--14.0
	FE Data			

APPENDIX C – REFERENCES

Xiao, F., Hulsey, J. L., and Cheng, G. S., (2015), Multi-direction Bridge Model Updating using Static and Dynamic Measurement, Applied Physics Research, Vol. 7, No. 1.

APPENDIX D – TRANSVERSE BEHAVIOR PRIOR TO MODEL MODIFICATIONS

The stiffness of the cross frame and support conditions affects load distribution in the transverse direction. In the report by HDR, Inc., five roller bearings did not fully connect with the superstructure, and HDR, Inc. removed those supports from their FEM (HDR, Inc., 2011).

During Phase 1 of this study, five displacement sensors were placed at those locations to measure the movement of the roller bearings in the vertical direction. In addition, eight strain sensors were installed on the diagonal members to measure the reaction of the supports and the stresses in the cross frames.

For one of the load test cases conducted on September 10, 2012, three heavily loaded trucks traveling side by side crossed the bridge at low speed (Hulsey, J.L., P. Brandon, and F. Xiao; 2012b).   The vertical movement of the five displacement sensors is shown in Figure D.1a–e. These graphs illustrate the response for an average of 50 data points over time for each of the five bearing locations.

According to the displacement sensor results, roller bearings 1, 3, and 4 have limited movement in the vertical direction. When compared with the other roller bearings, bearings 2 and 5 are more flexible in the vertical direction than the others are (Xiao and Hulsey, 2015).
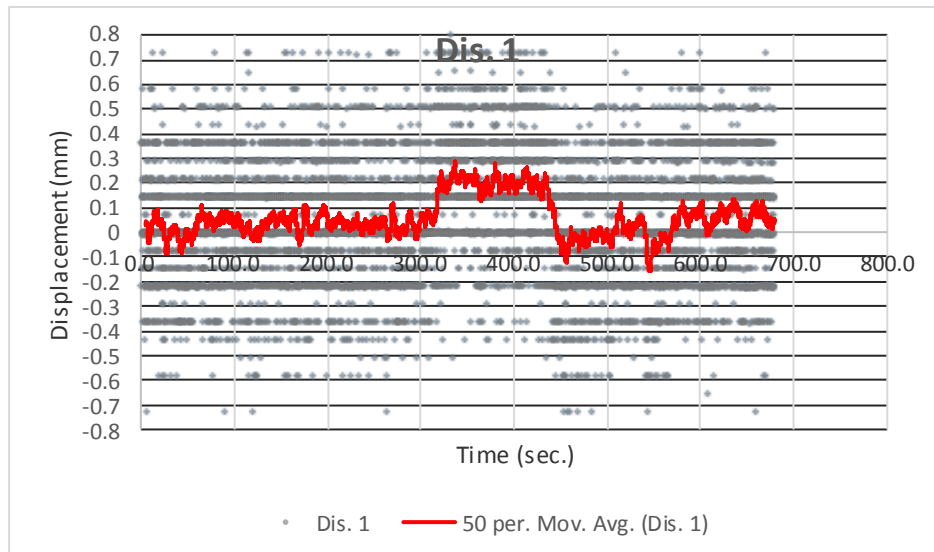
a. Vertical movement at displacement sensor 1
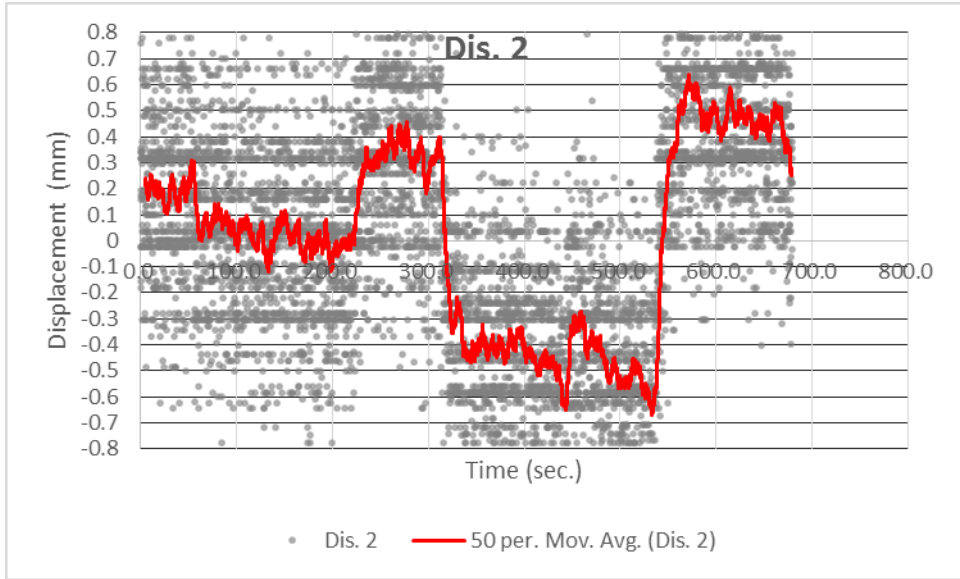
b. Vertical movement at displacement sensor 2
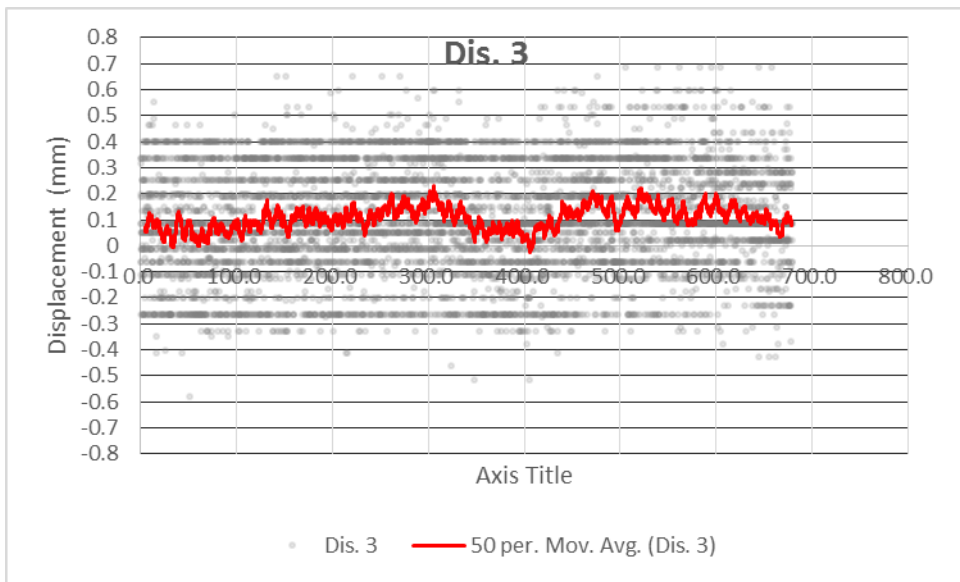
c. Vertical movement at displacement sensor 3
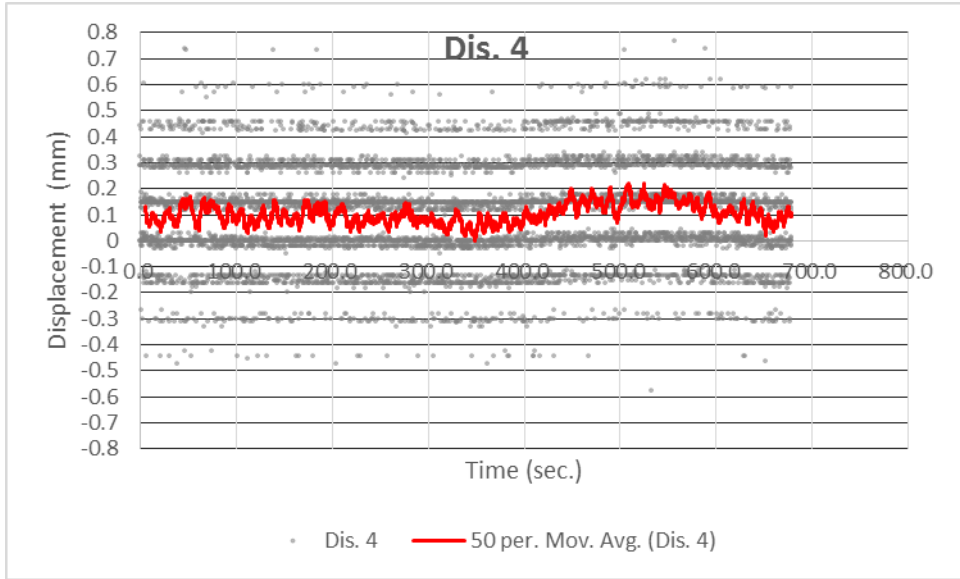
d. Vertical movement at displacement sensor 4
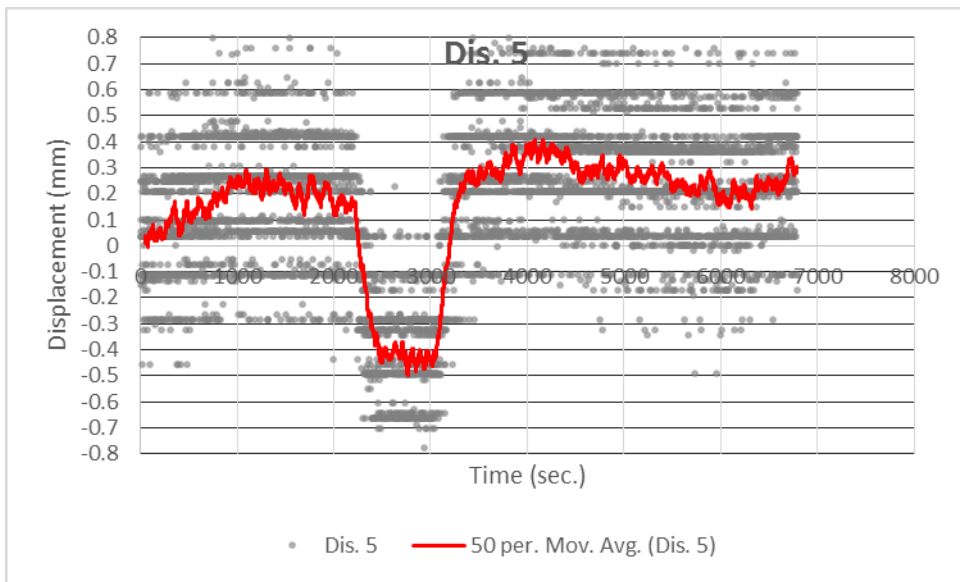
e. Vertical movement at displacement sensor 5

Figure D.1 Vertical movement at 5 unconnected bearing supports

In order to evaluate the distribution of reaction forces for a given load, eight strain sensors were installed (Phase 1) on the cross frame at the five unconnected roller support locations (Hulsey et al., 2012a). Tables D.1 and D.2 and Figures D.2 and D.3 show the stress results of measured and the calculated stress using the model prior to being updated. Table D.1 and Figure D.2 show the stress results when two parallel trucks stop above Pier 3. Table D.2 and

Figure D.3 show stress results when two parallel trucks stop over Pier 5. The details of these load tests are presented in the AUTC Load Test Report (Hulsey et al., 2012b). Sensor numbers and their locations are presented according to the modifications that were made to the FEM in the transverse direction

Table D.1 Two trucks at Pier 3, before transverse modifications

Location	C7	C6	C5	C4
Measured Stress (psi)	-2,237	1,127	1,726	-2,021
HDR FEM Stress (psi)	-2,963	1,482	1,466	-2,898
Error (%)	-32.4	-31.5	15.1	-43.4

Table D.2 Two trucks at Pier 5 stress results before transverse updating

Location	C28	C27	C25	C24
Measured Stress (psi)	-2,171	-2,058	-376	-1,172
HDR FEM Stress (psi)	-2,184	-2,366	-2,305	-2,261
Error (%)	-0.6	-15.0	-512.3	-92.9
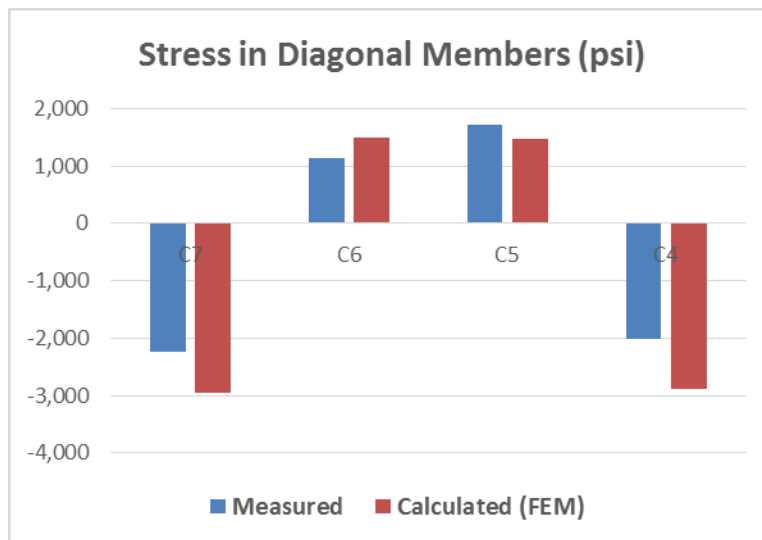
Figure D.2 Two trucks at Pier 3 stress results before FEM transverse modifications
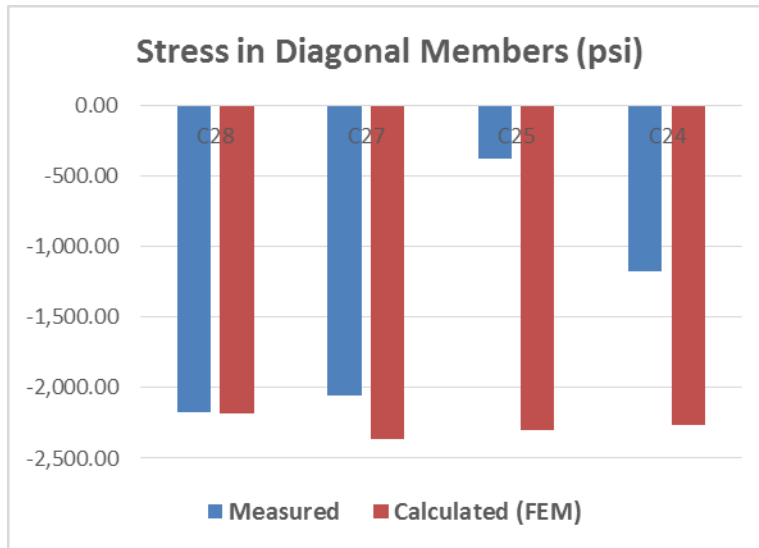
Figure D.3 Two trucks at Pier 5 stress results before transverse updating

APPENDIX D – REFERENCES

HDR, Inc. 2011. "Load Rating and Structural Assessment Load Rating Report – Bridge No. 255: Chulitna River Bridge."

Hulsey, J.L., P. Brandon, and F. Xiao. 2012b. "Structural Health Monitoring and Condition Assessment of Chulitna River Bridge: Load Test Report." Alaska Department of Transportation Research, Development, and Technology Transfer, Fairbanks, Alaska.

Xiao, F., Hulsey, J. L., and Cheng, G. S., (2015), Multi-direction Bridge Model Updating using Static and Dynamic Measurement, Applied Physics Research, Vol. 7, No. 1.

APPENDIX E – MODEL IMPROVEMENTS (TRANSVERSE DIRECTION)

Figures D.2 and D.3 show for the 2012 load tests that large errors existed between measured and calculated stresses in the cross frame. At Pier 3, the largest error was -43.4% in the cross frame. At Pier 5, the largest error was -512.3% (Hulsey, J.L., and F. Xiao, 2013). Figure D.1 indicates that bearings 1, 3, and 4 had limited movement. So the cross frame section may work as a semi-rigid support at those locations. As part of the model modifications, three spring supports were added at those locations. In order to reduce errors in the objective functions, the support spring stiffness and sectional properties of the cross frame were modified to more closely represent 1993 as-built conditions and behavior of this structure. Vertical spring support stiffness at locations 1, 3 and 4 are 1,200 kip/inch, 100 kip/inch, and 40,000 kip/inch, respectively. The cross frame truss section area was decreased to 0.8. The results for the modified finite element model (FEM) are shown in Tables E.1 and E.2 and Figures E.1 and E.2.

Table E.1 Two trucks at Pier 3 stress results after model modificatons (psi)

	C7	C6	C5	C4
Measured Stress (psi)	-2,237	1,127	1,726	-2,021
FEM Stress (psi)	-2,419	1,002	1,560	-2,106
Error (%)	-8.1	11.1	9.6	-4.2

Table E.2 Two trucks at Pier 5 stress results after model modificatons (psi)

	C28	C27	C25	C24
Measured Stress (psi)	-2,171	-2,058	-376	-1,172
FEM Stress (psi)	-1,8301	-1,0813	-2,027	-946
Error (%)	11.3	-17.0	-19.9	19.3
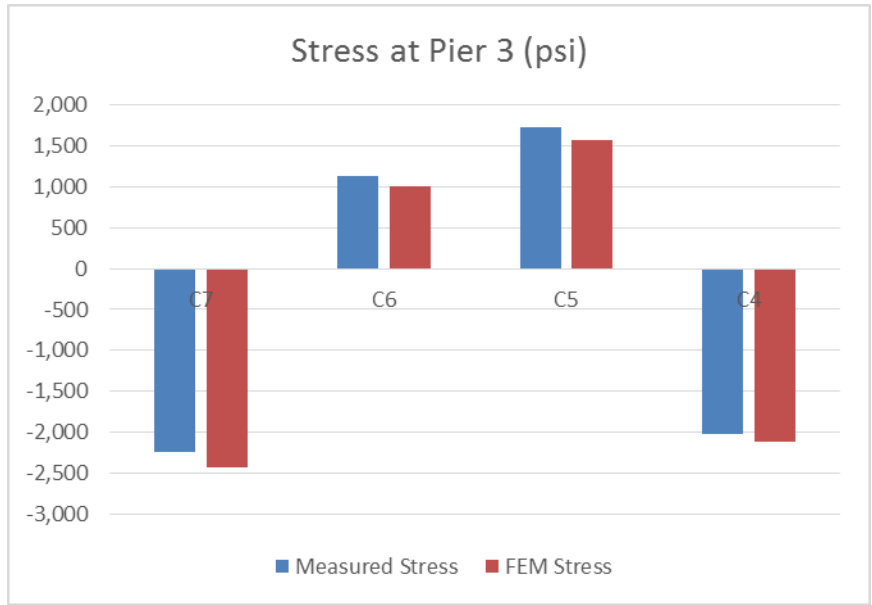
Figure E.1 Two trucks at Pier 3 stress results after model modifications
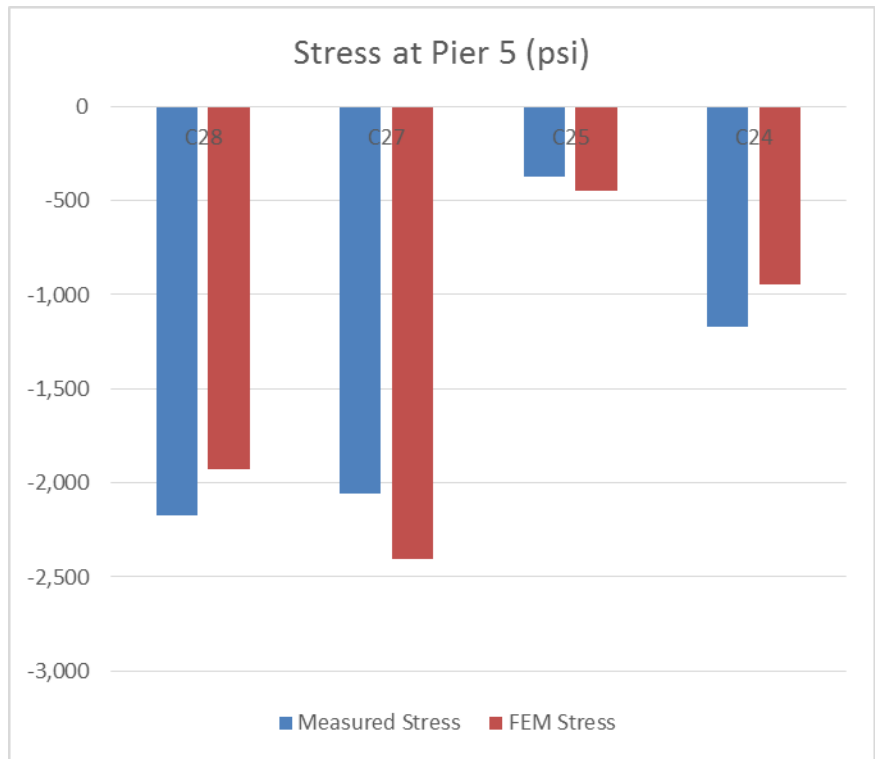
Figure E.2 Two trucks at Pier 5 stress results after model modifications

Following modification of the model, the largest error in the transverse direction decreased from -512.3% to -19.9%. Initially, five support bearings did not support the bridge (i.e., the superstructure was not in contact with the bearings). After the model was modified, bridge response was simulated with two bearings (Bearings 2 and 4) that were not in contact with the structure. At the other three bearing locations, the superstructure is modeled with vertical springs between the bearing support and the structure. The cross frames were found to be too stiff compared with the as-is condition (Xiao, Hulsey and Chen, 2015).

After the FEM was modified to more accurately represent the transverse behavior of the bridge, a comparison between experimental and calculated stresses were made for the various load tests that were run on September 10, 2012. For example, Tables E.3 and E.4 show for the middle of span 3, the difference in stresses between experimental and modified finite element values for girder flanges and the difference in stresses in the lower chord of the cross frame. These stresses are from a static load test in which three trucks side-by-side were on the bridge (see Figure E.3). The tables show that the stiffness of the three spring supports and the cross frame had limited influence on the longitudinal distribution of load.

Table E.3 Percent difference between FEM and experimental flange stresses mid-Span 3

Load Case	Location	1	2	3	4	5
	Sensor Number	R3	C9	C12	C15	L3
Top Flange	Field Measurement	-13.10	-13.50	-16.48	-17.69	-9.19
	FE Data					
Bottom Flange	Field Measurement	-6.58	0.71	5.43	4.26	-8.64
	FE Data					

Table E.4 Percent difference between FEM and experimental lower chord stresses mid-Span 3

Load Case	Location	1	2	3
	Sensor Number	R3	C9	C12
Top Flange	Field Measurement	-2.77	-5.24	-12.67
	FE Data			
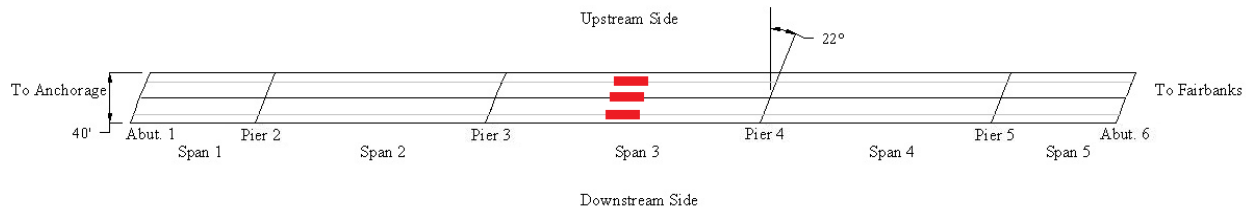
Figure E.3 Three trucks positioned on Span 3, southbound

After model modifications, the transverse structural response was evaluated for both local and global data. Using the improved model, global natural frequencies were calculated and compared with those that were measured with the portable accelerometers. Natural frequencies were calculated in three directions (vertical, longitudinal, transverse) and compared with the measured values (Table E.5). The largest error was 8.9% for the first mode in the longitudinal direction. Based on a comparison between test data and calculated values, it is clear that the modified FEM is sufficiently accurate. Ambient acceleration (global tests) tests were conducted in both 2012 and 2013 to determine if a change in structural behavior may have occurred. Table E.6 illustrates the bridge was stable for the year it was monitored.

Table E.5 Year 2012 natural rrequency difference; calibrated FEM

Mode	Field Measured (Hz)	FEM Results (Hz)	Difference (%)
Longitudinal Mode 1	1.500	1.367	8.9
Longitudinal Mode 2	2.190	2.044	6.7
Vertical Mode 1	2.846	2.756	3.2
Vertical Mode 2	3.224	3.348	-3.8
Vertical Mode 3	4.586	4.249	7.3
Transverse Mode 1	2.095	2.269	-8.3
Transverse Mode 2	2.346	2.542	-8.4
Transverse Mode 3	2.782	2.788	-0.2

Table E.6 Natural frequencies difference between 2012 and 2013

	2012 Ambient Test (Hz)	2013 Ambient Test (Hz)	FEM Calibrated Model
Longitudinal Mode 1	1.500	1.500	1.367
Longitudinal Mode 2	2.190	2.206	2.044
Vertical Mode 1	2.846	2.883	2.756
Vertical Mode 2	3.224	3.236	3.348
Vertical Mode 3	4.586	4.617	4.249

APPENDIX E – REFERENCES

Hulsey, J.L., and F. Xiao. 2013. "Mid-span Loading Report." Alaska Department of Transportation Research, Development, and Technology Transfer, Fairbanks, Alaska.

Xiao, F., Hulsey, J. L., and Cheng, G. S., (2015), Multi-direction Bridge Model Updating using Static and Dynamic Measurement, Applied Physics Research, Vol. 7, No. 1.

APPENDIX F – CORRELATION BETWEEN CALIBRATED MODEL AND EXPERIMENTAL DATA

Mid-Span 2: Static Load Test with Three Trucks

Three trucks were stopped side by side near the middle of Span 2. Strain sensors C3, C2, and C1 on the lower chords for the interior truss girder in Span 2 are presented for review and consideration. A small sample of the load tests is presented in Appendix G; details are presented elsewhere (Hulsey and Xiao, 2013; Hulsey et al., 2012b). These tests illustrate the correlation between the calibrated model and experimental data. Sensor locations can be seen on the sensor layout presented in Appendix H. Table F.1 and Figure F.1 show FEM local stresses and calculated local stresses from the measured local strains for a three-truck load test. These data show that errors for the selected samples presented herein are small.

Table F.1 Difference in mid-Span 2 loading condition

	C3	C2	C1
Measured Stress (psi)	2,006	1,994	2,091
updated FEM Stress (psi)	2,056	2,090	2,030
Error (%)	-2.5	-4.8	.9
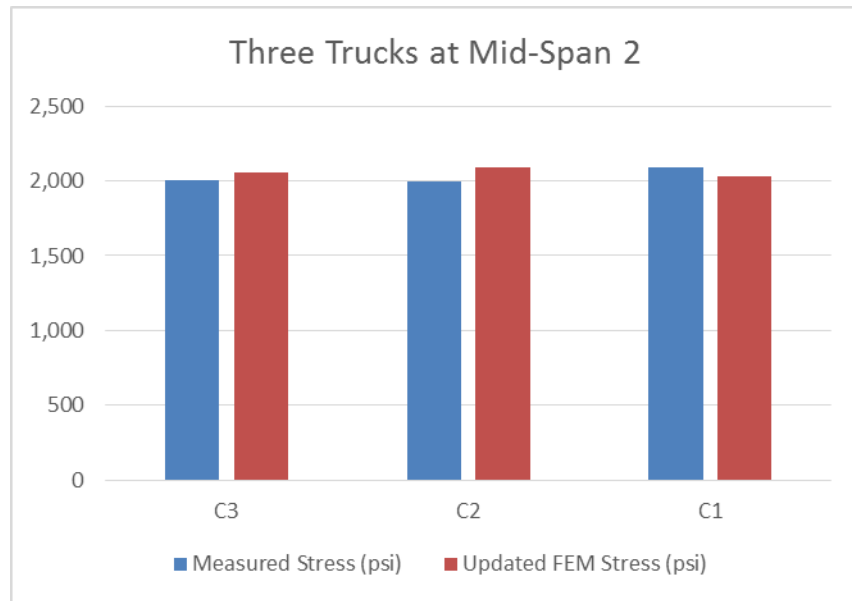
Figure F.1 Stress results in mid-Span 2 loading condition (psi)

Mid-Span 4 Loading Condition

Table F.2 Difference in mid-Span 4 three trucks side-by-side

	C23	C22	C21
Measured Stress (psi)	1,763	1,646	1,727
Updated FEM Stress (psi)	1,834	1,910	1,883
Error (%)	-4.0	-16.0	-9.0
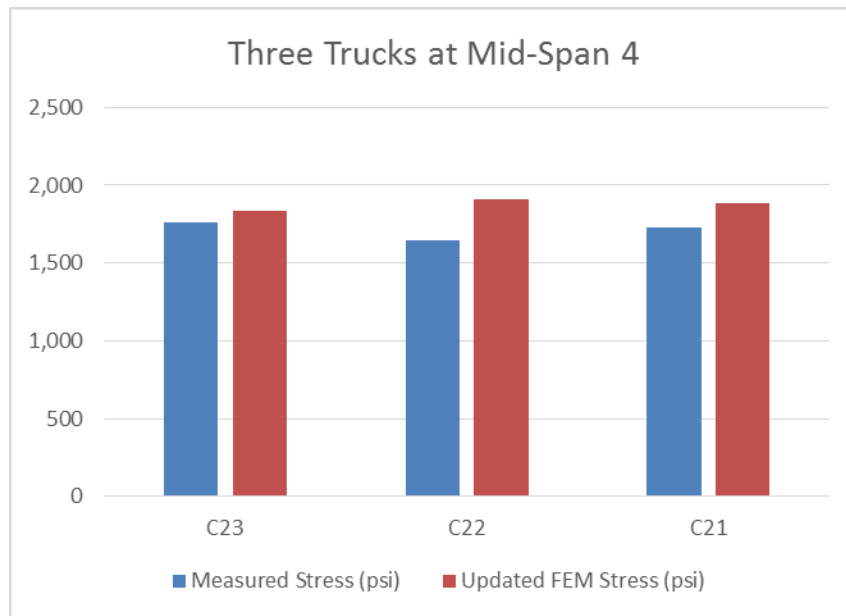
Figure F.2 Stress results for mid-Span 4 loading condition (psi)

APPENDIX F – REFERENCES

Hulsey, J.L., P. Brandon, and F. Xiao. 2012b. "Structural Health Monitoring and Condition Assessment of Chulitna River Bridge: Load Test Report." Alaska Department of Transportation Research, Development, and Technology Transfer, Fairbanks, Alaska.

Hulsey, J.L., and F. Xiao. 2013. "Mid-span Loading Report." Alaska Department of Transportation Research, Development, and Technology Transfer, Fairbanks, Alaska.

APPENDIX G – CALIBRATED FINITE ELEMENT MODEL

It is the purpose of this section to provide the reader with a three-dimensional view and details regarding the calibrated finite element model and its ability to virtually simulate the bridge response to load. The structure is 790 feet long; the bridge deck is 42 feet 2 inches wide. The bridge has 5 spans and is on a 22-degree skew. The model, which is shown in Figure G.1, uses SAP 2000 as the computer program; it has 4,697 nodal points, 4,615 frame elements, and 2,925 areas. The calibrated finite element model was used to compare calculated strains with measured values at the sensor locations, see Figure G2.   Table G.1 shows the number of elements that were used to accurately describe the current condition of this bridge. Tables G.2 and G.3 provide some of the known details about the bridge supporting system.
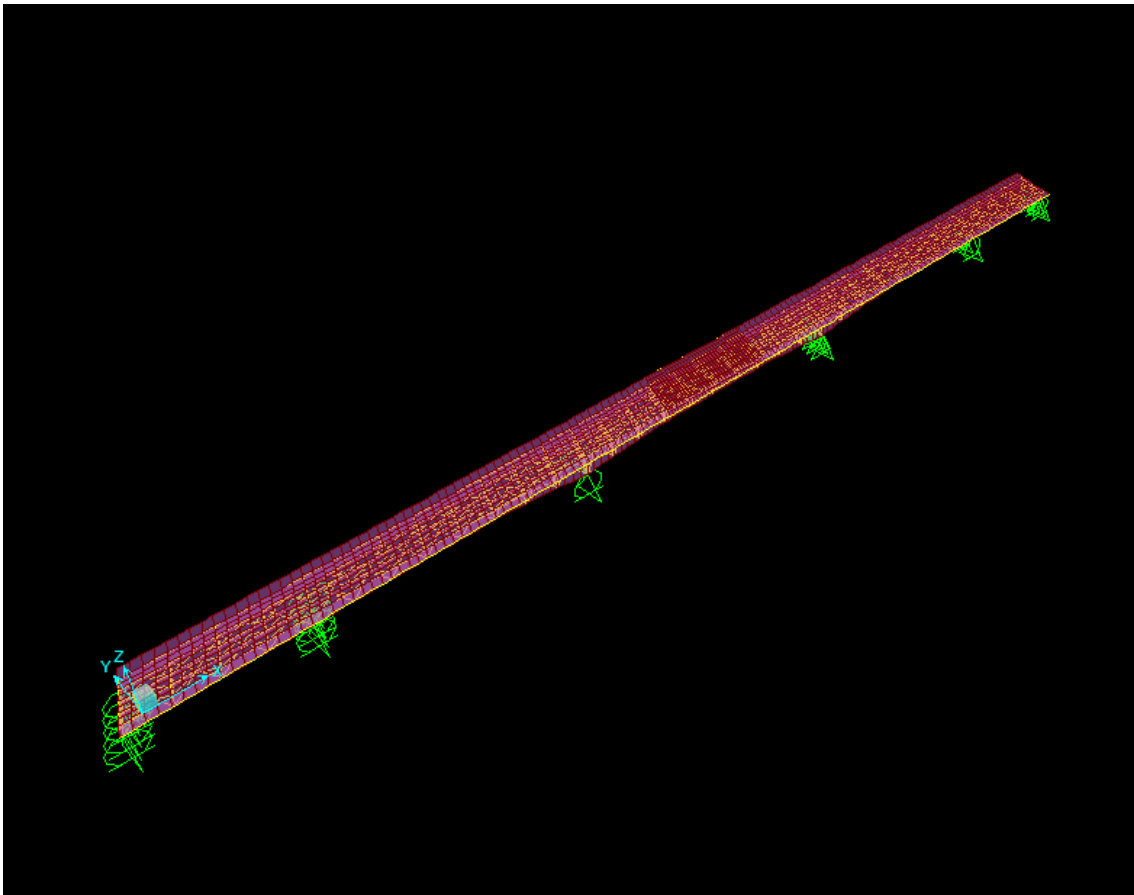
Figure G.1 Three-dimensional finite element model

Table G.1 Types of elements used in the model

Section		Element Type
Deck		Shell
Truss		Frame
Stringer	Web	Shell
	Flange	Frame
Girder	Web	Shell
	Flange	Frame

Table G.2 As-built support condition

	Abutment 1	Pier 2	Pier 3	Pier 4	Pier 5	Abutment 6
West Girder	Roller	Roller	Rollers	Fixed	Roller	Roller
West Truss	Roller	Roller	Roller	Fixed	Roller	Roller
Center Truss	Roller	Roller	Roller	Fixed	Roller	Roller
East Truss	Roller	Roller	Roller	Fixed	Roller	Roller
East Girder	Roller	Roller	Roller	Fixed	Roller	Roller

Table G.3 Calibrated FEM support condition

	Abutment 1	Pier 2	Pier 3	Pier 4	Pier 5	Abutment 6
West Girder	Roller	Roller	Rollers	Fixed	Roller	Roller
West Truss	Roller	Roller	100 kips/in	Fixed	Unconnected	Roller
Center Truss	Roller	Roller	Unconnected	Fixed	Roller	Roller
East Truss	Roller	Roller	1200 kip/in	Fixed	40,000 kips/in	Roller
East Girder	Roller	Roller	Roller	Fixed	Roller	Roller

Note: Bearing supports with a gap
    Location 1: Spring support stiffness is 1200 kip/inch in vertical direction.
    Location 3: Spring support stiffness is 100 kips/inch in vertical direction.
    Location 4: Spring support is 40,000 kips/inch in vertical direction.
    Locations 2 and 5: At these locations, the bridge is not connected to the supports.

Chulitna River Bridge Sensor Layout
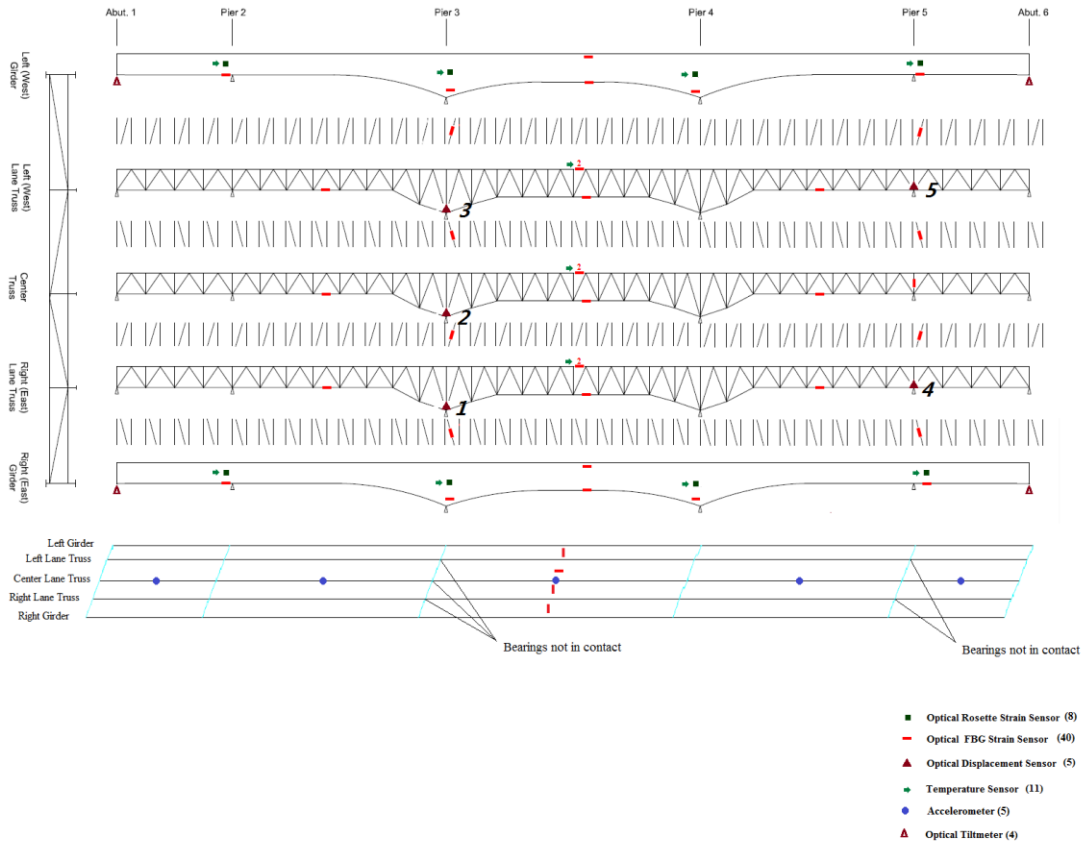
Figure G.2 Sensor layout and location for five bearing supports with a separation

APPENDIX H – SENSOR LAYOUT

The structural health monitoring system chosen for the Chulitna River Bridge had 73 sensors that were selected in collaboration with ADOT&PF Bridge Design. The sensor layout was to assist in evaluating the load distribution through the structure. Details of the sensor layout are published elsewhere (Xiao et al., 2012). Figures H.1- H.3 and Table H.1 shows the sensor layout used to study the response of this bridge.
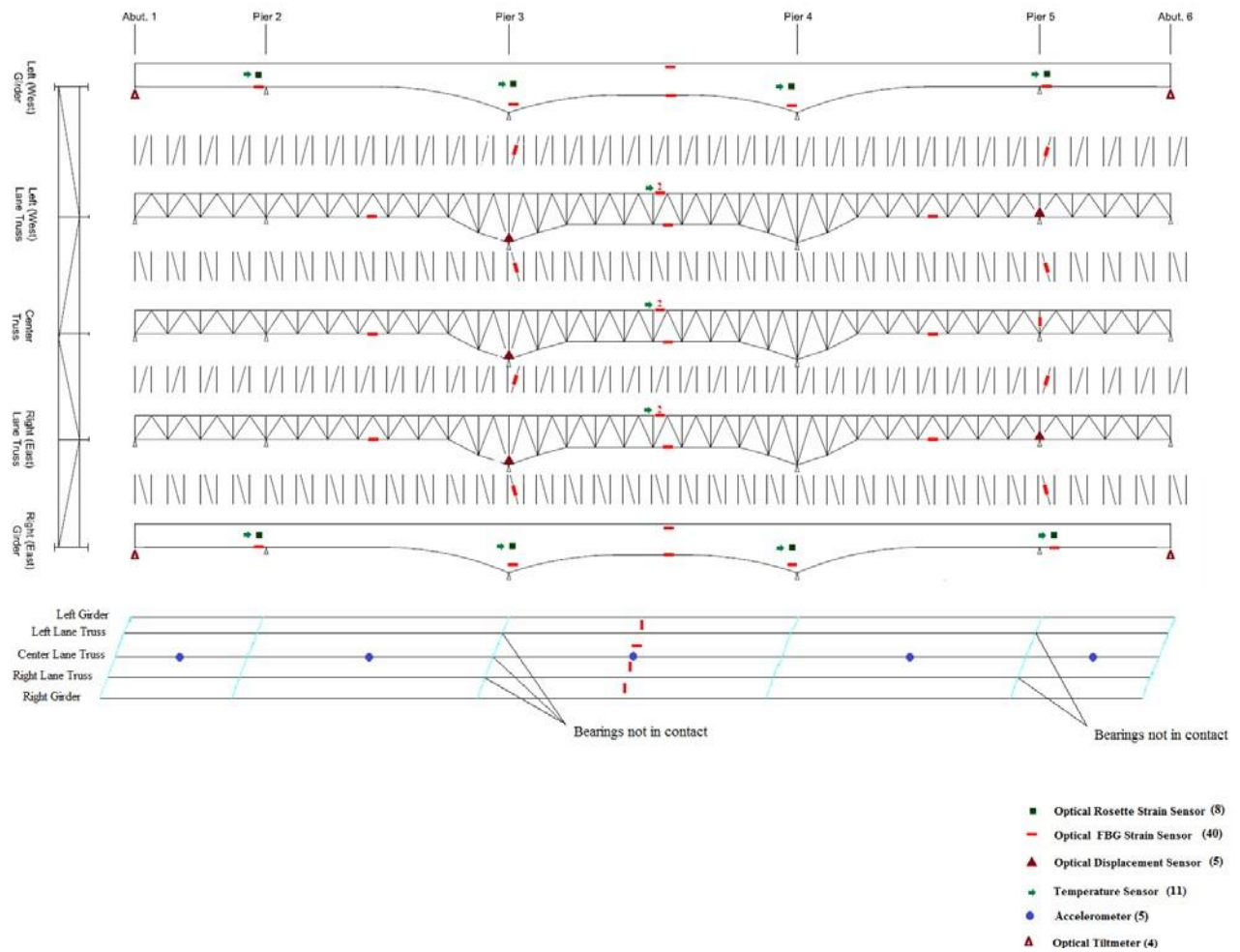
Figure H.1 Sensor layout

Table H.1 Summary of sensors

Sensor and Locations	Number of Sensors
Rosette Strain sensors	8
Strain Sensors on the Girders	12
Strain Sensors on the Composite Trusses	16
Strain Sensors on the Concrete Duck Strain	4
Sensor on the Diagonal Members	8
Accelerometers	5
Displacement Sensors	5
Temperature Sensors	11
Tilter meters	4
Total	73

Figure H.2 Sensor layout providing strains in C1–C3
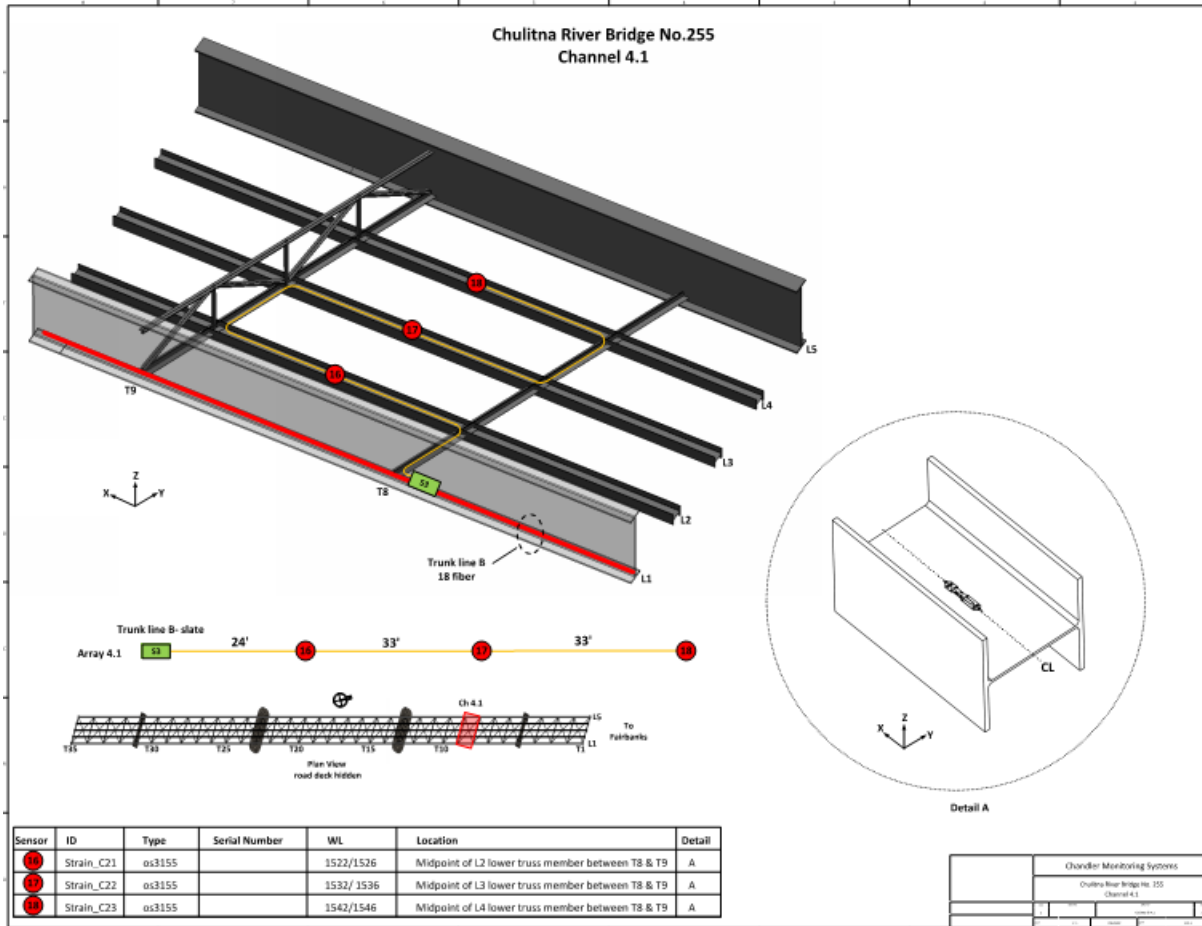
Figure H.3 Sensor layout providing strains in C21–C23

APPENDIX H – REFERNCES

Xiao, F., G. S. Chen, and J.L. Hulsey. 2012. "Experimental Investigation of a Bridge Under Traffic Loadings." *International Conference on Frontiers of Mechanical Engineering, Materials and Energy (ICFMEME 2012)*, Dec. 20, Beijing, China.

APPENDIX I – LOAD TESTING

A finite element model of the Chulitna River Bridge was calibrated to Phase 1, September 2012 experimental truck load data; August 2012 Phase 1 ambient vibration test data, and May 2013 Phase 2 ambient vibration test data. The details of the 2012 loads are reported elsewhere (Xiao et al., 2012; Hulsey et al., 2012b; Hulsey et al., 2013a, 2013b; Xiao et al., 2014).

The tests selected to calibrate the bridge behavior were as follows:

- Phase 1 – August 2012 Ambient tests to find global frequency data

- Phase 1 – September 10, 2012, load tests
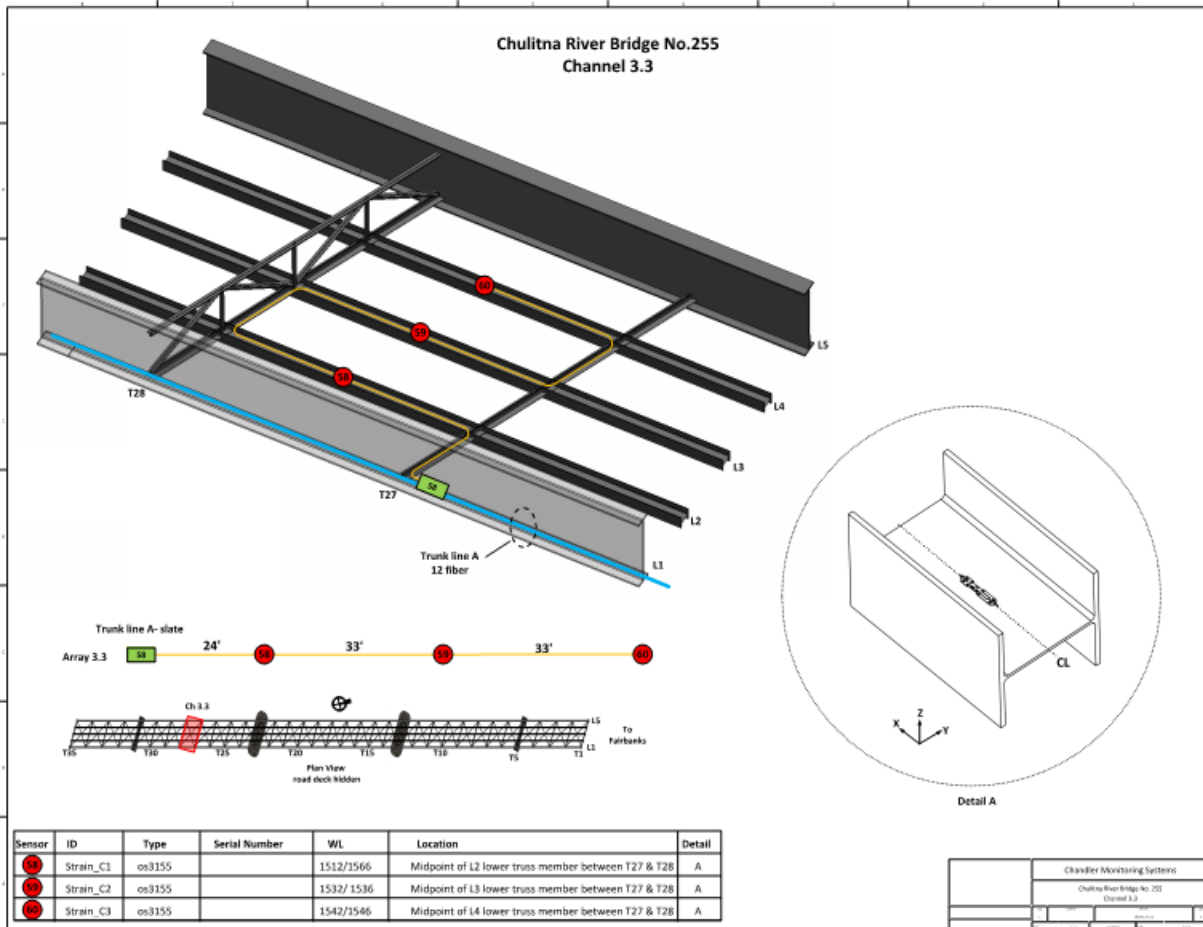
  o Local data from the two truck static loading (Trial 1);

  o Local data for the three truck static loading (Trial 17); and

  o Local data for the three truck dynamic loading (Trial 6);

- Phase 2 – May 2013 Ambient tests to find global frequency data

Appendix I is presented to provide the reader an understanding of the data used to calibrate the finite element model.

Phase 1

Global test data: In August 2012, "ambient" tests were conducted to evaluate the natural frequency response of the Chulitna River Bridge. These test results provided a baseline for the bridge condition in August 2012. In this report, the resulting experimental test data obtained from the "ambient" tests are referred to as *global* test data

Local test data: On September 10, 2012, the Chulitna River Bridge was load tested with three loaded dump trucks. Seventeen different combinations of these trucks were used to statically and dynamically load test the bridge. The structural health monitoring system (SHMS) was calibrated on September 9, 2012, in preparation for monitoring the structural response to these loaded trucks. Using SHMS, 73 sensors were monitored during testing. The sensor information (strains, temperatures, tilt displacements, and accelerations) are referred to as *local* experimental data.

Phase 1 – Ambient Tests (August 2012)

Short-term dynamic field vibrational tests were conducted on the Chulitna River Bridge in August 2012. An ambient free-decay response approach was used to estimate dynamic properties of the bridge. Stationary and dynamic tests were used to measure the acceleration response of the bridge at different locations and in different orientations during excitation caused by pedestrian traffic and ADOT&PF boom trucks. Natural frequencies were identified and characterized by fast Fourier transform (FFT) methods. The bridge's first eight tested modes are 1.50, 2.20, 2.85, 3.23, and 4.58 Hz. Of these tested modes, 2.85, 3.23, and 4.58 Hz are vertical modes and 1.50 and 2.20 Hz are longitudinal modes; the remaining three are transverse modes.

Fifteen portable single-axis accelerometers were used for the ambient tests (see Figs. I.1 and I.2). The accelerometers were located at piers and mid-spans. Because Spans 2, 3, and 4 are longer, more data collection points were placed in these spans. All accelerometers were set in a line along the center width of the deck on the flat clean driving surface. Vertical, transverse, and longitudinal accelerations were measured. In each, data were collected three times. Testing details are provided elsewhere (Xiao et al., 2012; Hulsey et al., 2012b; Hulsey et al., 2013a, 2013b; Xiao et al., 2014).
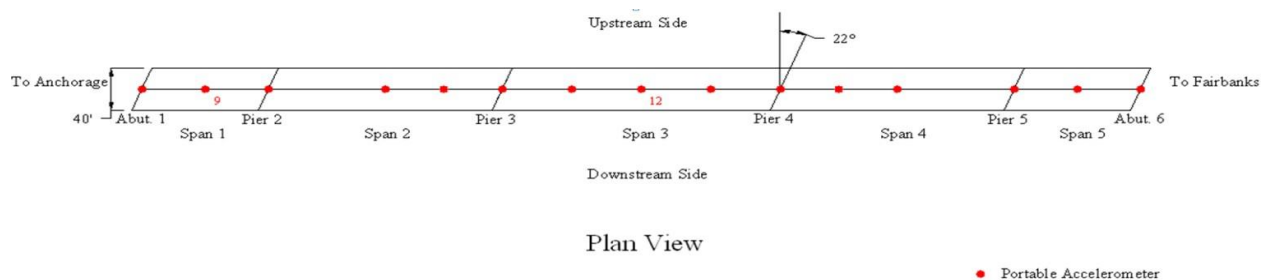
Figure I.1 Portable accelerometer location and number

Portable accelerometer
(15 were used)

As part of the conducted dynamic test, an FHWA's A-30 boom truck was used to excite
the bridge. Traffic control was used to stop pedestrian traffic in an effort to isolate the
excitation caused by the test vehicle. The bridge was closed to traffic and conditions were
non-windy during the dynamic test. Every effort was made to reduce the influence of erroneous
input. The A-30 boom truck crossed the bridge from Fairbanks to Anchorage (traveling south) in
the upstream lane at a speed of 45 mph (Fig. I.3). The bridge was kept closed while the bridge's
excitation was monitored until vibration was totally damped out.

Figure I.3 A-30 boom truck traveling north for the dynamic ambient test

During the study, the research team found that recorded modal parameters are sensitive to sensor locations. Some locations are sensitive; some are not. At some locations, the output is too small to offer specific modal information reliably, or the information is too weak to be identified. As such, optimization was needed. In practice, multiple point measurements are needed to guarantee reliability and robustness of the measurement.

In the following figures and tables, the two most sensitive data locations were chosen for processing. Figure I.4 shows the FFT of a typical measured acceleration signal in the vertical direction in the middle of Span 3 (Point 12). Figure I.4 shows that multiple peaks exist with f_1=1.50 Hz, f_2=2.85 Hz, and f_3=3.23 Hz dominating.
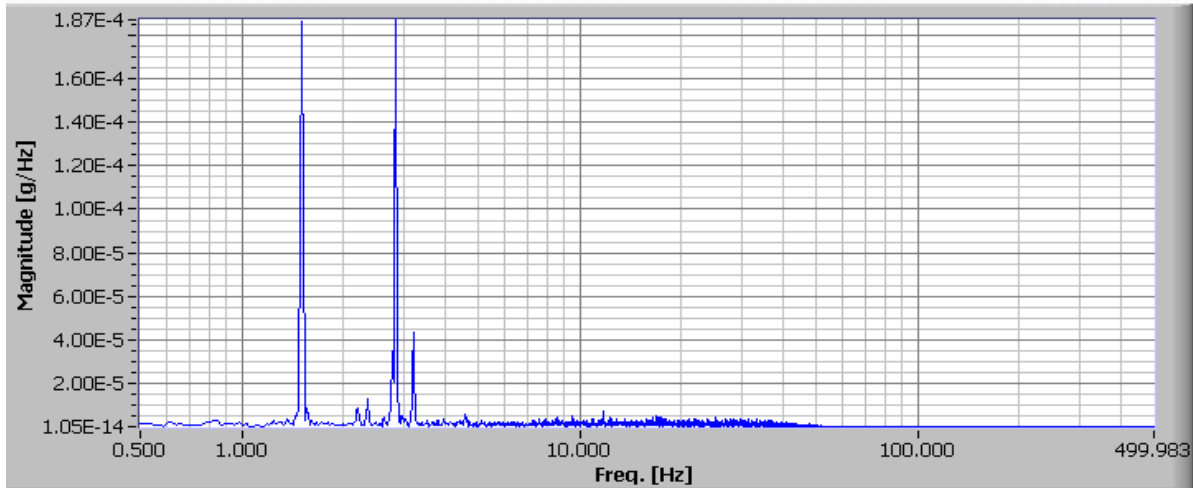
Figure I.4 FFT for measured vertical acceleration (middle of Span 3; Point 12)

Figure I.5 shows the FFT of a typical measured acceleration signal in the vertical direction in the middle of Span 1 (Point 9). In Figure I.5, multiple peaks are seen, with f_{1a}=1.50 Hz, f_{2a}=2.20 Hz, f_{3a}=2.85 Hz, and f_{4a}=4.58 Hz dominating.
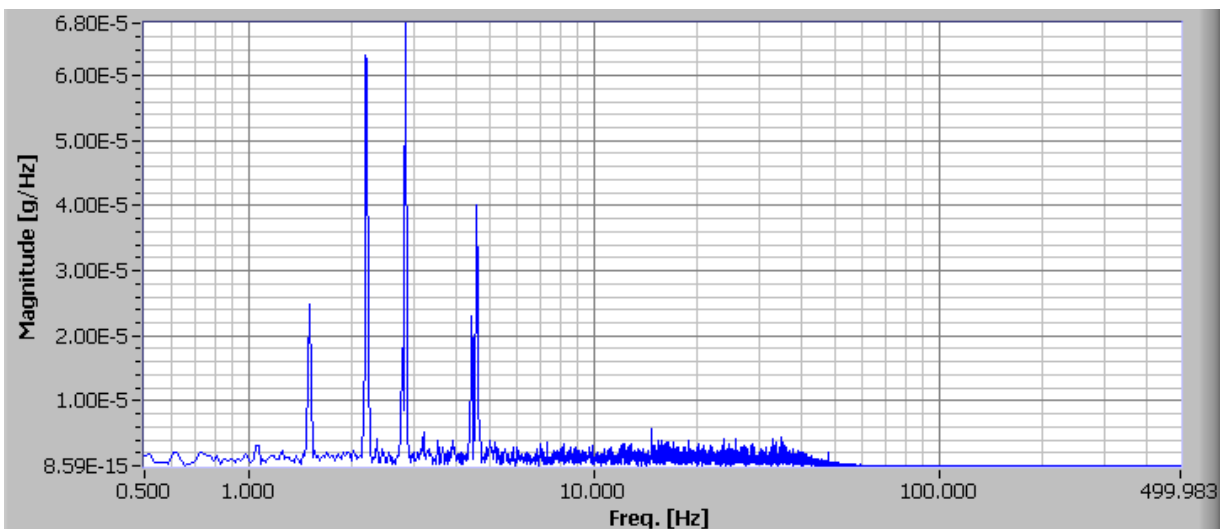
Figure I.5 FFT for measured vertical acceleration (middle of Span 1, Point 9)

Phase 1 – SHMS: Description of ADOT&PF Dump Truck Loading

Three ADOT&PF dump trucks were used to load test the Chulitna River Bridge on September 10, 2012. Prior to the load test, three empty ADOT&PF dump trucks were provided

for testing the bridge. Each truck-trailer was weighed and measured. Then, the trailers were loaded with sand and the truck-trailers were weighed (this is the load prior to testing). At the end of the day on September 10, after the load test, the three loaded ADOT&PF dump trucks were again weighed. This data provided the researchers with a record of the change in weight over the 8-hour test period. Axle weights were measured with calibrated portable scales provided by the ADOT&PF (see Figs. I.6 and I.7).

Figure I.6 Axle weight measured by the wheel load scales

Figure I.7 Wheel load scales WL 101

Tables I.1 through I.3 are ADOT&PF dump truck measurement results from the portable weigh station. Load 1 was measured on September 9, the night before the load test, and Load 2 was measured on September 10, after the load test. Axle 1 is the steering axle (Fig. I.8).

Table I.1 Truck No. 36188 measurement results

	Measurement	Axle 1	Axle 2	Axle 3	Axle 4	Axle 5	Gross weight (lb)	Axle width
Truck 36188 (Heading) 37438 (Trailer)	Axle distance	15'3"		4'6"	29'1"	4'2"		
	Axle weight (Empty)	13,050 lb	8,100 lb	7,900 lb	4,800 lb	5,050 lb	38,900	6'6"
	Axle weight (Loaded 1)	13,200 lb	18,300 lb	18,400 lb	15,950 lb	16,250 lb	82,100	
	Axle weight (Loaded 2)	13,000 lb	18,400 lb	18,900 lb	16,650 lb	15,150 lb	82,100	

Table I.2 Truck No. 35752 measurement results

	Measurement	Axle 1	Axle 2	Axle 3	Axle 4	Axle 5	Gross weight (lb)	Axle width
Truck 35752 (Heading) 31526 (Trailer)	Axle distance	15'4"		4'5"	29'9"	4'1"		
	Axle weight (Empty)	12,550 lb	9,400 lb	9,100 lb	5,900 lb	5,800 lb	42,750	
	Axle weight (Loaded 1)	12,100 lb	18,850 lb	18,500 lb	15,500 lb	15,650 lb	80,600	6'6"
	Axle weight (Loaded 2)	12,300 lb	18,850 lb	18,850 lb	14,800 lb	15,550 lb	80,350	

Table I.3 Truck No. 36195 measurement results

	Measurement	Axle 1	Axle 2	Axle 3	Axle 4	Axle 5	Gross weight (lb)	Axle width
Truck 36195 (Heading) 36580 (Trailer)	Axle distance	16'9"		4'8"	28'9"	4'1"		
	Axle weight (Empty)	13,150 lb	7,950 lb	7,900 lb	3,200 lb	6,000 lb	38,200	
	Axle weight (Loaded 1)	13,350 lb	18,400 lb	18,100 lb	13,750 lb	16,650 lb	80,250	6'8"
	Axle weight (Loaded 2)	13,350 lb	18,450 lb	18,300 lb	12,150 lb	18,100 lb	80,350	

Figure I.8 Axle location

Phase 1 – Load Testing With Trucks

Heavily Loaded Trucks Load Test Trial 1 (Static)

In this test, two trucks were positioned with the trucks side-by-side (parallel) to the 22
angle (Fig. I.9) southbound at 1 mph. At each pier and at mid-span, the trucks were stopped for
30 seconds to record static response data. Truck No. 36188 was on the downstream side of the

bridge and Truck No. 36195 was on the upstream side of the bridge (see Tables I.1 through I.3 for truck weight, axle width, and axle spacing.
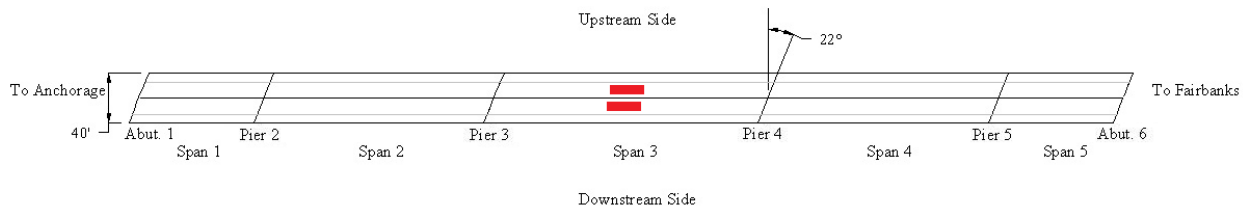

Figure I.9 Two trucks side-by-side and positioned in Span 3

In Trial 1, the ADOT&PF trucks used for testing were stopped and positioned in the middle of Span 3 (between Piers 3 and 4). The front axles were located 369 feet from the south abutment (Abutment 1) (see Figs. I.10 and I.11). A finite element analysis for these same load conditions was conducted. The local calculated strains and displacements were compared with the experimental SHMS response data
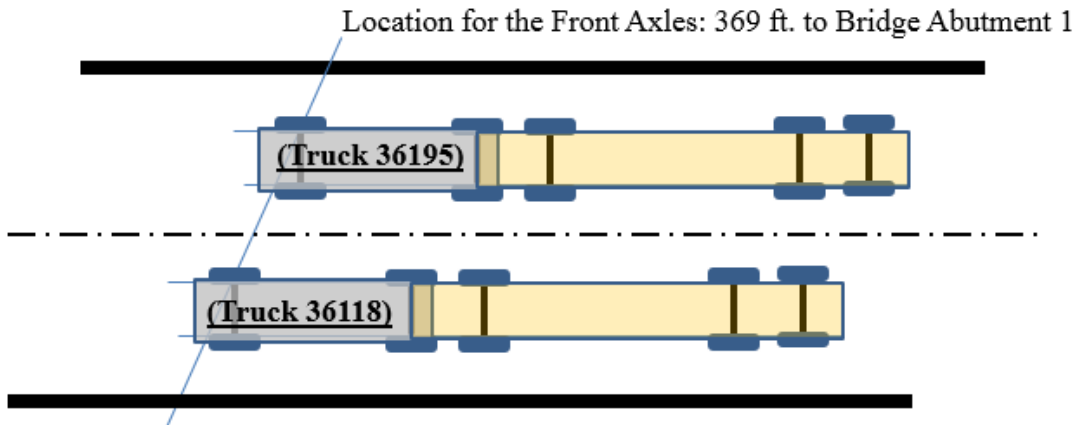

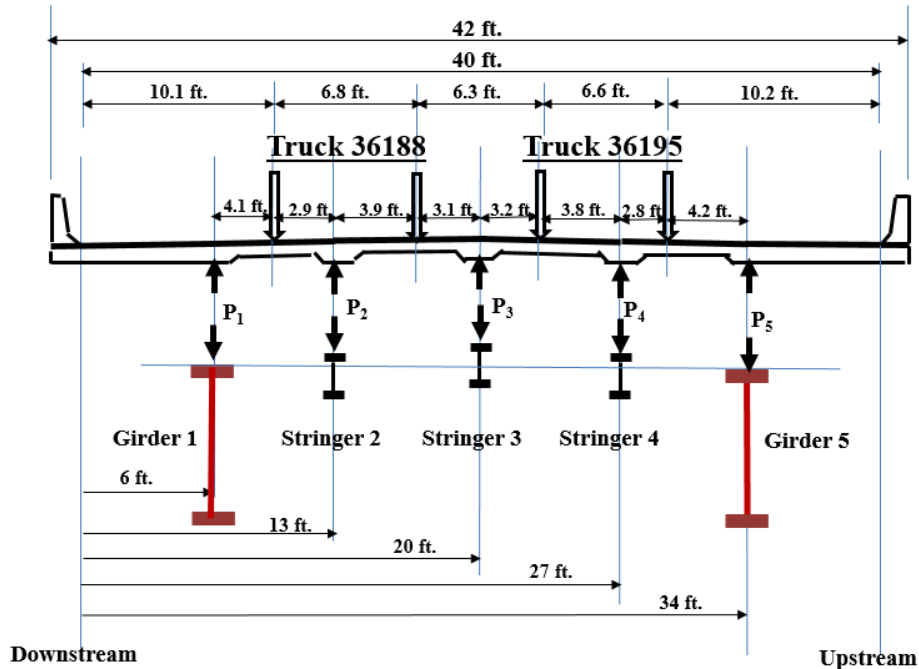Figure I.10 Plan view of two trucks at mid-Span 3 southbound

Figure I.11 Cross-sectional elevation view of two trucks at mid-Span 3

Heavily Loaded Trucks Load Test Trial 17 (Static)

Three trucks traveled parallel to the 22-degree skew angle of the bridge. Truck No. 36195 was on the upstream side of the bridge (Fig. I.12). The ADOT&PF loaded trucks moved southbound at 1 mph. Static tests were conducted by stopping the trucks for no less than 30 seconds at several pre-determined locations along the length of the bridge. In Trial 17, three trucks were positioned at mid-span of Span 3 (see Figs. I.13 and I.14). The FEM calculated values were compared with local SHMS data. Truck No. 36188 was on the middle of the bridge, and Truck No. 35752 was on the downstream side of the bridge (see Figs. I.13 and I.14).
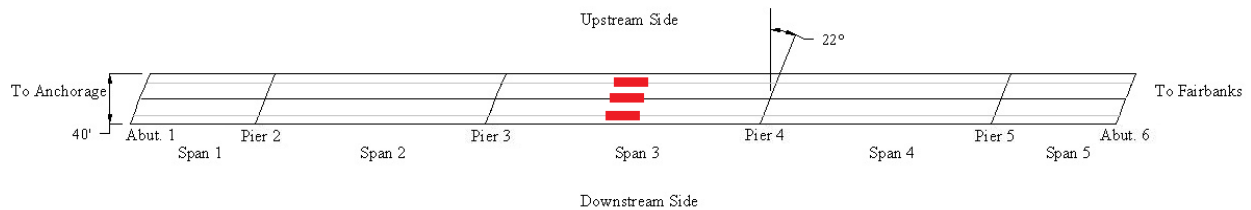

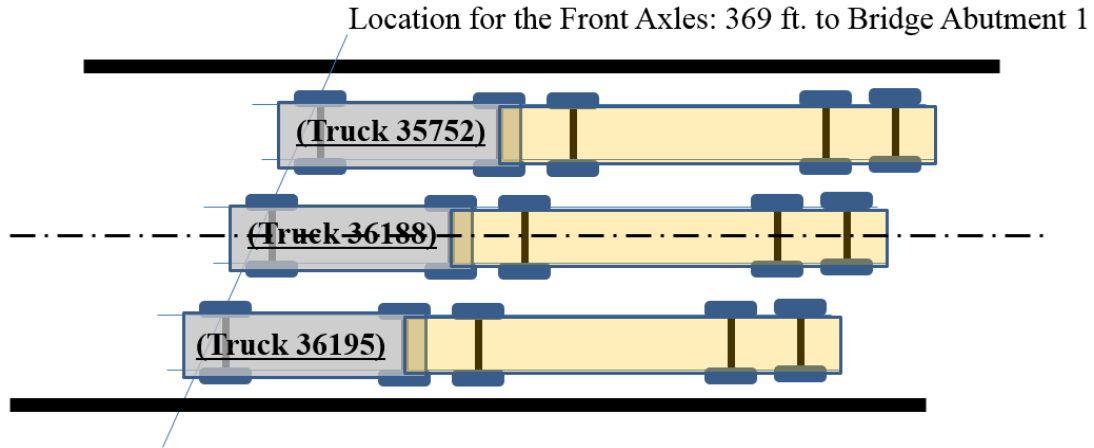Figure I.12 Three trucks side by side

Location for the Front Axles: 369 ft. to Bridge Abutment 1

(Truck 35752)

(Truck 36188)

(Truck 36195)

Figure I.13 Plan view of three trucks at mid-span southbound

42 ft.

40 ft.

Truck 36188   Truck 36195   Truck 36195

2.4 ft. 4.4 ft.   3.3 ft. 3.3 ft.   4.3 ft. 2.3 ft.

P_1 P_2 P_3 P_4 P_5

Girder 1   Stringer 2   Stringer 3   Stringer 4   Girder 5

6 ft.

13 ft.

20 ft.
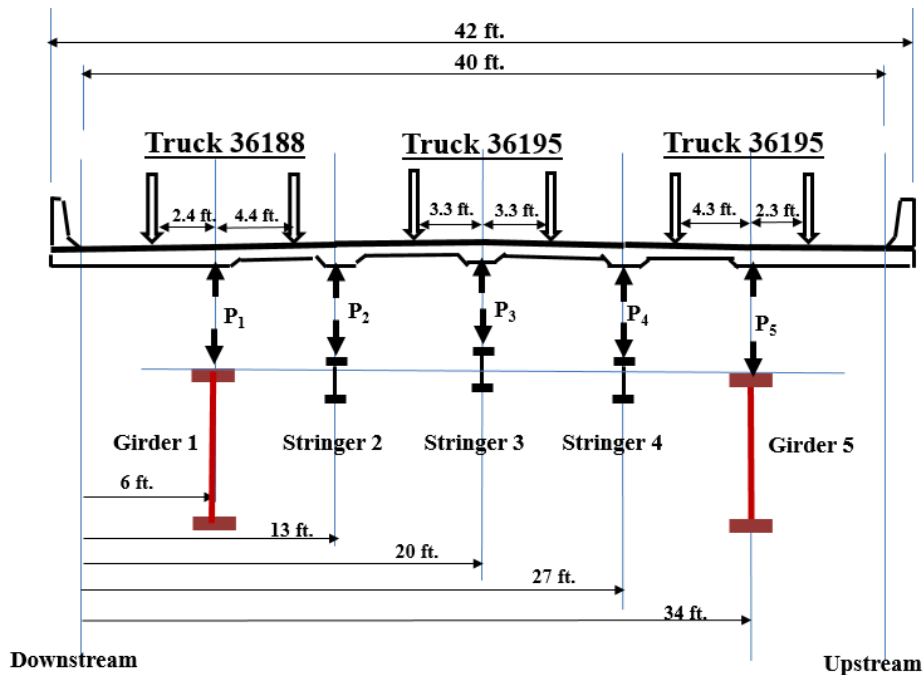
27 ft.

34 ft.

Downstream   Upstream

Figure I.14 Vertical view of three trucks at mid-span

Heavily Loaded Trucks Load Test Trial 6 (Dynamic)

In this test, the three ADOT&PF test trucks traveled side by side (Fig. I.15) heading north. Truck No. 36195 was in the downstream lane. Truck No. 36188 was in the middle lane and Truck No. 35752 was in the upstream lane. The research team requested that the drivers travel as fast as they could safely cross the bridge. The ADOT&PF truck drivers selected a speed of 15 mph for this series of dynamic tests (see Fig. I.15 and Table I.4).
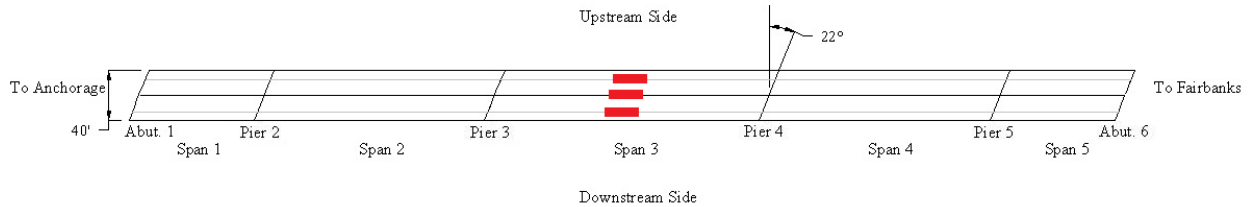
Figure I.15 Three trucks side by side

Table I.4 Dynamic load test Trial 6

| Test	Type	Direction	Description	Time
6	Dynamic	North	Start Test	10:51
			End Test	10:53

Phase 2 – Ambient Tests (May 2013)

The ambient type of test is inexpensive and quick and can be done while performing a routine bridge inspection. The idea is to conduct this test to determine if the bridge may have undergone a significant change that is not visible to the naked eye. This tool does not provide the necessary information to identify a localized crack. It will provide an overall global evaluation in which a stiffness change has occurred. If a sufficient number of higher modes are monitored, it may be plausible to identify some localized issues. Additional research to evaluate the benefit of some of these issues is needed.

In May 2013, a second "ambient" test was conducted on the bridge; the first test was in August 2012. Again, fifteen portable accelerometers were placed in a line along the length of the bridge and located down the center of the driving surface (see Fig. I.16).
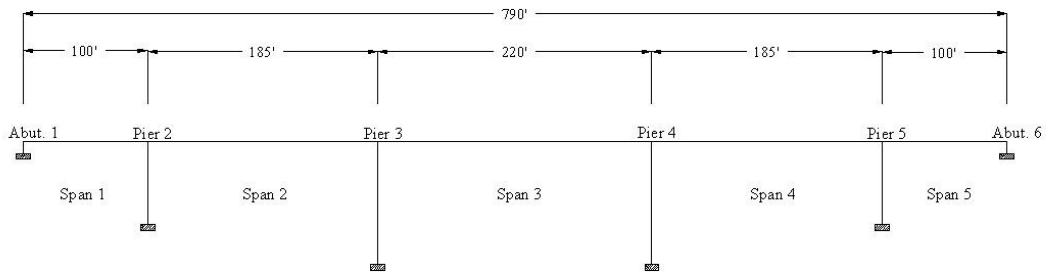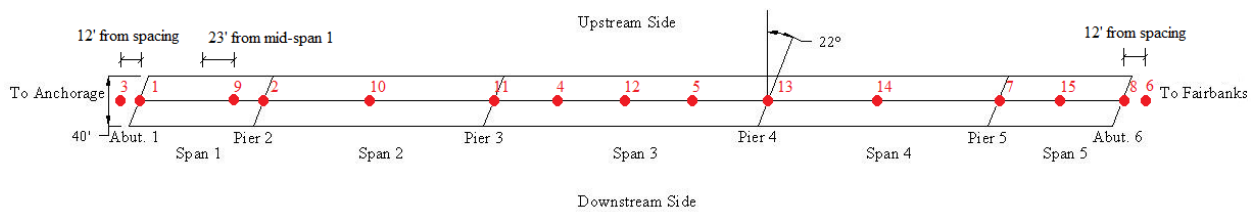
Figure I.16 Accelerometer layout

At the request of the research team, two test trials were performed. For Trial 1, ADOT&PF was asked to drive the boom truck across the bridge at 45 mph; this was done from north to south. Traffic was kept off the bridge while the acceleration data were recorded. This test was followed by Trial 2. In this case, ADOT&PF drove the boom truck from south to north. The testing procedure was repeated, in that traffic was stopped until the acceleration data were recorded. Table I.5 provides a summary of the difference between the 2012 and 2013 natural frequency data for the longitudinal and vertical modes. Table I.5 shows very little difference between natural frequencies in 2012 versus 2013. This result illustrates that there was effectively no structural change in the behavior of the Chulitna River Bridge between 2012 and 2013. Table I.6 shows a correlation between the 2013 experimental data and the FEM calculated values.

Table I.5 Natural frequencies difference between 2012 and 2013 test results

	2012 Ambient Test (Hz)	2013 Ambient Test (Hz)	100*[(Old-New)/Old]
Longitudinal Mode 1	1.500	1.500	0.000
Longitudinal Mode 2	2.190	2.206	-0.731
Vertical Mode 1	2.846	2.883	-1.300
Vertical Mode 2	3.224	3.236	-0.372
Vertical Mode 3	4.586	4.617	-0.676

Table I.6 Natural frequencies difference between 2013 field measurement and updated model

Mode	Field Measurement (Hz)	FEM Results (Hz)	Difference (%)
Longitudinal Mode 1	1.500	1.367	8.9
Longitudinal Mode 2	2.206	2.044	7.3
Vertical Mode 1	2.883	2.756	4.4
Vertical Mode 2	3.236	3.348	-3.46
Vertical Mode 3	4.617	4.249	8.0

APPENDIX I – REFERENCES

Hulsey, J.L., F. Xiao, and G.S. Chen. 2013a. "Structural Health Monitoring of an Alaska Bridge." *6th International Conference on Structural Health Monitoring of Intelligent Infrastructure*, Hong Kong, December.

Hulsey, J.L., F. Xiao, and G.S. Chen. 2013b. "Structural Health Monitoring System Optimization for a Bridge." *6th International Conference on Structural Health Monitoring of Intelligent Infrastructure*, Hong Kong, December.

Xiao, F., G.S. Chen, and J.L. Hulsey. 2014. "Experimental investigation of a bridge under traffic loading." *Advanced Materials Research*, 875–877: 1989–1993.

APPENDIX J – A FUTURISTIC APPROACH TO CALIBRATING A FINITE ELEMENT MODEL

It is suggested that the next stage of research should include optimization methodology for modifying and refining computer models. For example, consider the test data show that a change has occurred to the bridge. So, what is the bridge experiencing? Is there a significant crack, a change in the support conditions, or something else?

The procedure will first involve converting the finite element model (FEM) that supposedly represents what is believed to be the bridge structure into a mathematical model. More objective functions will be selected from static and dynamic tests. For the purpose of future research, the finite element model will represent the base line and any changes will be referred to as model updates. As more variables are used and revised, it is appropriate to divide the structural system into small sections according to bridge spans. The objective functions and variables will be set within reasonable ranges. The optimized results will be calculated based on mathematical optimization methods. Additional objective functions and variables will ensure the reliability of the updated model. The latest reasoning is that with this approach, an optimized updated method can be used to intelligently control the objective functions so that achieving convergence is reasonable and errors between experimental and calculated data will be small. After completing the FEM optimization scheme, the largest error between calculated and experimental data is expected to be between 2% and 5% for global values and between 5% and 15% for local values (Xiao and Hulsey, 2015).

The outcome of this approach will be a FEM of the bridge's current condition. This model will provide a virtual behavioral response of the bridge for a given set of loading conditions. As more data are taken, the differences between experimental and calculated data should be routinely checked. If the bridge's latest measured experimental (SHMS) local data are different than predicted or if the latest measured global data are different, the health of the bridge has likely changed and a further investigation should be conducted. In this process, the model would be updated to search on the cause of the change in the health of the structure. Once the cause is identified, the Agency can evaluate the overall importance of the change of condition. If no warnings are identified, then this approach may be performed in conjunction with bridge inspection.

APPENDIX J – REFERENCES

Xiao, F., Hulsey, J. L., and Cheng, G. S., (2015), Multi-direction Bridge Model Updating using Static and Dynamic Measurement, Applied Physics Research, Vol. 7, No. 1.